JOURNAL OF CLINICAL MICROBIOLOGY, Feb. 2008, p. 792–795 Vol. 46, No. 2
0095-1137/08/$08.00+0 doi:10.1128/JCM.01470-07

Dual-Reporter Phenotypic Assay for Human Immunodeficiency Viruses[▽]

Keiko Kajiwara, Eiichi Kodama,* Yasuko Sakagami, Takeshi Naito, and Masao Matsuoka

Laboratory of Virus Immunology, Institute for Virus Research, Kyoto University, 53 Kawaramachi, Shogoin, Sakyo-ku, Kyoto 606-8507, Japan

Received 22 July 2007/Returned for modification 27 September 2007/Accepted 5 December 2007

We have established a novel human immunodeficiency virus (HIV) tandem-reporter assay using HIV receptor-transduced NP-2 cells with long terminal repeat-controlled β-galactosidase, inserted internal ribosome entry site, and secretary alkaline phosphatase genes. This assay allows users to detect replication of clinical isolates, indicating its useful application as an HIV phenotypic assay.

Assays for detecting the emergence of resistant variants, as well as evaluating clinical efficacy, provide useful information regarding chemotherapy for human immunodeficiency virus (HIV) infection. To date, two types of assay systems have been developed and approved, namely, genotypic and phenotypic assays (13, 31). Genotypic assays detect genetic mutations that are associated with drug resistance and lead to rapid and sensitive detection of the emergence of resistant variants (9), although they only provide estimated resistance profiles (16, 30). Lists of significant resistance-associated mutations in reverse transcriptase (RT), protease, and envelope genes are maintained by some organizations and Universities, such as the International AIDS Society-USA (http://iasusa.org/resistance mutations); Los Alamos National Laboratory, Los Alamos, NM (http://resdb.lanl.gov/Resist_DB); and the Stanford University, Stanford, CA (http://hivdb.stanford.edu/index.html). PCR-based genotypic assays are heavily dependent on the primers used. Therefore, some biases must unfortunately be presumed, since most primer-matched sequences are preferentially amplified, resulting in some discordance with phenotypic assays (21, 33) that are time-consuming and require tedious procedures because isolation of replication-competent viruses is required. To date, phenotypic assays for clinical isolates have been mainly performed in experiments with a p24 production assay in phytohemagglutinin-stimulated peripheral blood mononuclear cells (27, 32, 34).

For more rapid and simple phenotypic assays, recombinant viruses containing the region responsible for resistance have been utilized instead of isolated viruses (14, 18, 35). However, since protease resistance mutations are introduced simultaneously with gag mutations (4, 25), cloning of the entire gag and protease coding region is occasionally required. Recently, mutations for 3′-azido-3′-deoxythymidine (AZT) resistance have been identified in the connection and/or RNase H subdomain (5, 7, 26), which no commercially available genotypic and phenotypic assays include for the analysis. Moreover, the mechanism of resistance to a fusion inhibitor, enfuvirtide, is a complex issue, since mutations in not only the gp41 coding region (6, 24) but also the V3 region (29) and the CD4-binding site (2) of gp120 influence the susceptibility, indicating that patient-derived viruses are ideally required for evaluation of drug susceptibility.

Recently, Hachiya et al. established a simple and rapid phenotypic assay using MAGIC5 cells (CCR5-transduced MAGI cells) (11). This system efficiently isolates clinical HIV variants and has proven to be useful for evaluating drug susceptibility (12). However, the expression of transduced receptors on MAGIC5 cells declines during prolonged culture, as described for MAGI cells (17). Therefore, in order to obtain HIV isolates efficiently and perform the assay, relatively fresh cells are required. More recently, we established a tetrazolium-based colorimetric assay for monitoring replications of not only CXCR4 (X4)-tropic but also CCR5 (R5)-tropic HIVs and drug susceptibilities (17). We reported that NCK45 cells stably express HIV receptors on their cell surface and provide reproducible results (17). Since this assay depends on the cytopathic effect induced by HIV, it appears to be insufficient for assessing infections with no or a few cytopathic variants. Furthermore, it requires 7 days of culture to obtain the drug susceptibility. In the present study, we have established a novel single long terminal repeat (LTR)-driven tandem two-reporter system using the internal ribosome entry site (IRES) (15), which enables the evaluation of drug susceptibility within 2 days for various HIVs, including clinical isolates.

To construct an LTR-driven reporter vector, an amplified LTR region (the −138 to +89 region of the transcriptional start site of HIV-1 molecular clone pNL4-3) was inserted into pβgal-Basic (Clontech Laboratories, Inc., Palo Alto, CA) between the NheI and HindIII sites (pLTR-βgal). The 5′ region (HindIII to EcoRV) of the β-galactosidase gene was replaced with the responsible β-galactosidase fragment with nuclear localization signal sequence (MPKKKRK) amplified from genomic DNA of MAGI cells (20). Fragments of IRES and secretory alkaline phosphatase (SEAP) were amplified from pIRES2-EGFP and pSEAP2-Basic (Clontech Laboratories, Inc.), respectively. A puromycin-resistance gene (Puro^r) under the control of the phosphoglycerate kinase promoter as a selection marker was inserted at the SalI site of the vector (pLTR-β-Gal/SEAP-Puro^r), as shown in Fig. 1A. All fragments were verified by sequencing.

The pLTR-β-Gal/SEAP-Puro^r plasmid was transfected into NCK45 cells (CD4, CXCR4, and CCR5-transduced NP-2 cells

* Corresponding author. Mailing address: Laboratory of Virus Immunology, Institute for Virus Research, Kyoto University, 53 Kawaramachi, Shogoin, Sakyo-ku, Kyoto 606-8507, Japan. Phone and fax: 81-75-751-3986. E-mail: ekodama@virus.kyoto-u.ac.jp.

▽ Published ahead of print on 19 December 2007.

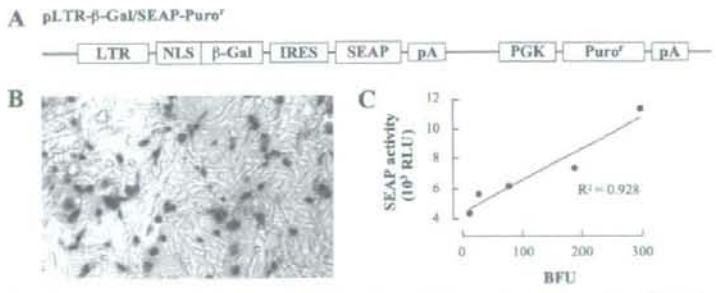

FIG. 1. Establishment of a cell line with β-galactosidase (β-Gal) and SEAP genes driven by an LTR. (A) Schematic diagram of the vector used in the present study, which simultaneously expresses genes for β-Gal and SEAP under the control of the HIV-1 LTR promoter (pLTR-β-Gal/SEAP-Puro^r). The enhancer region (positions −138 to +89) of the LTR, the nuclear localization signal (NLS) derived from the T-antigen of simian virus 40, the IRES, the phosphoglycerate kinase promoter (PGK), and the polyadenylation signal (pA) are also shown. (B) Microscopic image of X-Gal-stained NCK45-β-Gal/SEAP cells at 48 h after virus inoculation. (C) Correlation between β-Gal and SEAP activities in culture supernatants. NCK45-β-Gal/SEAP cells were infected with HIV at various infectious doses and incubated for 48 h. Culture supernatants were examined for their SEAP activities and expressed as relative right units (RLU). BFU, blue-cell-forming units.

derived from a glioma) (17, 36) to detect intracellular Tat expression through the LTR-driven tandem reporter genes. At 48 h after transfection, the cells were cultured in Dulbecco modified Eagle medium (Sigma, St. Louis, MO) supplemented with 5% heat-inactivated fetal calf serum, 0.5 mg of G418 disulfate (Nacalai Tesque, Kyoto, Japan)/ml, 0.2 mg of hygromycin B (Calbiochem, La Jolla, CA)/ml, and 10 μg of puromycin (Sigma)/ml and designated NCK45-β-Gal/SEAP cells. The expression levels of receptors on NCK45 cells confirmed by a flow cytometer (17) were 97, 83, and 99%, while those on H9 cells as a control were 65, 73, and 0.3% for CD4, CXCR4, and CCR5, respectively.

To evaluate anti-HIV agents, NCK45-β-Gal/SEAP cells (5×10^4 cells/ml) in Dulbecco modified Eagle medium-based culture medium supplemented with 5% fetal calf serum, penicillin, and streptomycin were seeded onto 96-well plates. On the following day, the cells were inoculated with sample viruses at 60 blue-cell-forming units (BFU)/well, incubated for 48 h, and then cultured in the presence of various concentrations of drugs. After 48 h of culture, the cells were fixed with 1% formaldehyde and 0.2% glutaraldehyde for 3 min, washed three times with phosphate-buffered saline, and incubated with X-Gal (5-bromo-4-chloro-3-indolyl-β-D-galactopyranoside) for 2 h (Fig. 1B). To evaluate the SEAP activities, the culture supernatants were harvested and analyzed by using a Great EscAPe SEAP chemiluminescent detection kit (BD Biosciences Clontech, Palo Alto, CA) according to the manufacturer's protocol. Samples were measured by using a Wallac 1450 MicroBeta Jet Luminometer (Perkin-Elmer, Wellesley, MA). For comparison, MAGI-CCR5 cells were analyzed as previously described (17).

The activities of various anti-HIV agents toward NCK45-β-Gal/SEAP cells were compared to those in the MAGI assay. The BFU and SEAP activities were well correlated with the viral input (Fig. 1C; correlation coefficient $R^2 = 0.928$). We tested various anti-HIV agents (Table 1): DS5000, an adsorption inhibitor; AZT and 2′,3′-dideoxycytidine (ddC), RT inhibitors; T-140 (37), a CXCR4 antagonist; and TAK-779, a CCR5 antagonist (1). The antiviral activities of the compounds determined by each reporter in NCK45-β-Gal/SEAP cells were comparable to those obtained using MAGI cells, although some were statistically significant (Table 1). Intracellular nucleoside/nucleotide metabolisms, especially thymidine kinase (10), and expression levels of receptors (19) may alter the 50% effective concentrations of the AZT and CCR5 antagonists, respectively.

NCK45-β-Gal/SEAP cells also supported the replication of various clinical isolates, as well as laboratory strains. The clin-

TABLE 1. Comparison of anti-HIV activities in MAGI and NCK45-β-Gal/SEAP cells

Compound	Target	Mean EC_{50} (μM)[a] ± SD						CC_{50} (μM)[b] (NCK45-β-Gal/SEAP)
		$HIV\text{-}1_{IIIB}$			$HIV\text{-}1_{Ba\text{-}L}$			
		MAGI	NCK45-β-Gal/SEAP		MAGI	NCK45-β-Gal/SEAP		
			β-Gal	SEAP		β-Gal	SEAP	
DS5000	gp120	0.14 ± 0.025	0.076 ± 0.026	0.07 ± 0.0034	0.36 ± 0.052	0.49 ± 0.069	0.42 ± 0.15	>100
AZT	RT	0.031 ± 0.013*	0.0043 ± 0.0022	0.0035 ± 0.0007	0.05 ± 0.029	0.0035 ± 0.0007	0.0094 ± 0.0063	>100
ddC	RT	0.4 ± 0.16	0.53 ± 0.12	0.42 ± 0.14	0.48 ± 0.17	0.72 ± 0.067	0.67 ± 0.2	>100
T-140	CXCR4	0.006 ± 0.0006	0.006 ± 0.0002	0.0025 ± 0.0008	>100	>100	>100	>100
TAK-779	CCR5	>100	>100	>100	0.003 ± 0.0019*	0.035 ± 0.0088	0.027 ± 0.0098	>100

[a] EC_{50}, 50% effective concentration. Data represent mean values of at least three independent experiments. $HIV\text{-}1_{IIIB}$ and $HIV\text{-}1_{Ba\text{-}L}$ utilize CXCR4 (X4) and CCR5 (R5) as coreceptors, respectively. *, The EC_{50} values obtained from MAGI and NCK cells (both β-galactosidase and SEAP) were statistically significant (Student *t* test, $P < 0.01$).

[b] CC_{50}, 50% cytotoxic concentration. The CC_{50} was determined by the MTT method after 2 days exposure of compounds as described previously (11).

TABLE 2. Drug susceptibility against HIV clinical isolates in MAGI and NCK45-β-Gal/SEAP cells

Compound	Cell line	Detection	EC_{50} (μM)[a]					
			KMT/R5X4	IVR405/R5X4	IVR406/R5X4	IVR409/R5X4	IVR416/R5X4	IVR417/R5
DS5000	MAGI	β-Gal	0.54	0.43	0.18	0.51	0.16	1.4
	NCK45-β-Gal/SEAP	β-Gal	0.6	0.22	0.14	0.46	0.22	1.9
		SEAP	0.28	0.27	0.19	0.28	0.16	1.5
AZT	MAGI	β-Gal	0.0027	>1.0	0.68	0.055	0.046	0.0033
	NCK45-β-Gal/SEAP	β-Gal	0.0038	>1.0	1.0	0.061	0.018	0.004
		SEAP	0.0044	>1.0	0.41	0.032	0.013	0.0015
ddC	MAGI	β-Gal	1.3	0.55	1.4	1.2	1.0	1.3
	NCK45-β-Gal/SEAP	β-Gal	1.0	0.32	1.0	1.3	0.75	0.79
		SEAP	2.0	0.24	2.1	1.5	0.52	0.77

[a] EC_{50}, 50% antiviral effective concentration. Amino acid substitutions in the RT region were as follows: none for KMT; M41L/E44D/D67G/V118I/Q151M/L210W/T215Y for IVR405; M41L/E44D/D67N/V118I/M184I/L210W/T215Y for IVR406; M41L/E44D/M184V/L210W/T215Y for IVR416; and D67N/V106AV/M184V/T215F for IVR407. Coreceptor usage is indicated in each subheading after the slash: R5X4, CCR5 and CXCR4 dualtropic virus; R5, CCR5-tropic virus.

ical isolates used in the present study were kindly provided by Y. Maeda (Kumamoto University School of Medicine, Kumamoto, Japan) and S. Oka (AIDS Clinical Center, International Medical Center of Japan, Tokyo, Japan). The drug susceptibilities of not only R5-tropic isolates but also X4-tropic and dualtropic isolates were comparable to those in the MAGI assay (Table 2). IVR405 and IVR406 were highly resistant to AZT, whereas IVR409 and IVR416 showed moderate resistance to AZT, and KMT and IVR417 were susceptible to AZT. These susceptibilities were confirmed by the MAGI assay.

In the present study, we established an IRES-mediated tandem-reporter assay using NCK45 cells for the rapid and simultaneous evaluation of the antiviral activities of compounds. This assay enables the evaluation of various HIV strains and clinical isolates within 3 days, including the cell preparation procedure. Secreted SEAP from HIV-infected NCK45 cells is also useful for monitoring the isolation of viruses without cell destruction and enables the continuous propagation of the isolates during isolation. Since NCK45-β-Gal/SEAP cells are susceptible to various viruses, including clinical strains, depending on the experimental purpose any HIV variants may be used for a reference virus, e.g., an isolate prior to the therapy. The LTR promoter for the dual reporters used in the present study includes four CpG methylation-sensitive sites, although Tat can transactivate the HIV-1 LTR regardless of the methylation state (3, 28). Thus, reporter genes in NCK45 cells are less affected by gene silencing.

Compared to the commercially available phenotypic assays, our established system may be useful especially for inhibitors targeting new molecules, including envelope proteins and integrase. A fusion inhibitor T-20 can suppress variants refractory to most of approved RT and protease inhibitors (22, 23). Both phenotypic and genotypic assays for T-20 are needed to evaluate the clinical outcome of patients with T-20-containing regimens. An approved CCR5 antagonist, maraviroc, may also suppress such refractory variants (8). Needless to say, to assess the drug susceptibility experimentally and/or clinically, a combination of established databases accumulated with various assays appears to be useful and important.

In conclusion, the tandem reporters β-Gal and SEAP can evaluate the exact viral infectivity and proportional LTR activation level by repetitive analyses of culture supernatants, respectively. This IRES-mediated tandem-reporter system may be applicable to other reporter genes, e.g., the luciferase gene. Thus, our assay system may provide simple, rapid and stable results for HIV phenotypic assays.

We thank J. Overbaugh for providing the HeLa-CD4/CCR5-LTR/β-Gal cells through the AIDS Research and Reference Reagent Program, Division of AIDS, National Institute of Allergy and Infectious Diseases (Bethesda, MD).

This study was supported in part by a grant for the Promotion of AIDS Research from the Ministry of Health and Welfare of Japan (to M.M. and E.K.); a grant for Research for Health Science Focusing on Drug Innovation from the Japan Health Science Foundation (to E.K.); and a grant from the Ministry of Education, Culture, Sports, Science, and Technology of Japan (to E.K.). K.K. and T.N. are supported by the 21st Century COE Program of the Ministry of Education, Culture, Sports, Science, and Technology.

REFERENCES

1. **Baba, M., O. Nishimura, N. Kanzaki, M. Okamoto, H. Sawada, Y. Iizawa, M. Shiraishi, Y. Aramaki, K. Okonogi, Y. Ogawa, K. Meguro, and M. Fujino.** 1999. A small-molecule, nonpeptide CCR5 antagonist with highly potent and selective anti-HIV-1 activity. Proc. Natl. Acad. Sci. USA **96:**5698–5703.
2. **Baldwin, C. E., and B. Berkhout.** 2006. Second site escape of a T20-dependent HIV-1 variant by a single amino acid change in the CD4 binding region of the envelope glycoprotein. Retrovirology **3:**84.
3. **Bednarik, D. P., J. A. Cook, and P. M. Pitha.** 1990. Inactivation of the HIV LTR by DNA CpG methylation: evidence for a role in latency. EMBO J. **9:**1157–1164.
4. **Brann, T. W., R. L. Dewar, M. K. Jiang, A. Shah, K. Nagashima, J. A. Metcalf, J. Falloon, H. C. Lane, and T. Imamichi.** 2006. Functional correlation between a novel amino acid insertion at codon 19 in the protease of human immunodeficiency virus type 1 and polymorphism in the p1/p6 Gag cleavage site in drug resistance and replication fitness. J. Virol. **80:**6136–6145.
5. **Brehm, J. H., D. Koontz, J. D. Meteer, V. Pathak, N. Sluis-Cremer, and J. W. Mellors.** 2007. Selection of mutations in the connection and RNase H domains of human immunodeficiency virus type 1 reverse transcriptase that increase resistance to 3′-azido-3′-dideoxythymidine. J. Virol. **81:**7852–7859.
6. **Cabrera, C., S. Marfil, E. Garcia, J. Martinez-Picado, A. Bonjoch, M. Bofill, S. Moreno, E. Ribera, P. Domingo, B. Clotet, and L. Ruiz.** 2006. Genetic evolution of gp41 reveals a highly exclusive relationship between codons 36, 38, and 43 in gp41 under long-term enfuvirtide-containing salvage regimen. Aids **20:**2075–2080.
7. **Delviks-Frankenberry, K. A., G. N. Nikolenko, R. Barr, and V. K. Pathak.** 2007. Mutations in human immunodeficiency virus type 1 RNase H primer grip enhance 3′-azido-3′-deoxythymidine resistance. J. Virol. **81:**6837–6845.
8. **Fatkenheuer, G., A. L. Pozniak, M. A. Johnson, A. Plettenberg, S. Staszewski, A. I. Hoepelman, M. S. Saag, F. D. Goebel, J. K. Rockstroh, B. J. Dezube, T. M. Jenkins, C. Medhurst, J. F. Sullivan, C. Ridgway, S. Abel, I. T. James, M. Youle, and E. van der Ryst.** 2005. Efficacy of short-term monotherapy

with maraviroc, a new CCR5 antagonist, in patients infected with HIV-1. Nat. Med. **11**:1170–1172.
9. **Frenkel, L. M., L. E. Wagner II, S. M. Atwood, T. J. Cummins, and S. Dewhurst.** 1995. Specific, sensitive, and rapid assay for human immunodeficiency virus type 1 *pol* mutations associated with resistance to zidovudine and didanosine. J. Clin. Microbiol. **33**:342–347.
10. **Gao, W. Y., R. Agbaria, J. S. Driscoll, and H. Mitsuya.** 1994. Divergent anti-human immunodeficiency virus activity and anabolic phosphorylation of 2′,3′-dideoxynucleoside analogs in resting and activated human cells. J. Biol. Chem. **269**:12633–12638.
11. **Hachiya, A., S. Aizawa-Matsuoka, M. Tanaka, Y. Takahashi, S. Ida, H. Gatanaga, Y. Hirabayashi, A. Kojima, M. Tatsumi, and S. Oka.** 2001. Rapid and simple phenotypic assay for drug susceptibility of human immunodeficiency virus type 1 using CCR5-expressing HeLa/CD4$^+$ cell clone 1-10 (MAGIC-5). Antimicrob. Agents Chemother. **45**:495–501.
12. **Hachiya, A., H. Gatanaga, E. Kodama, M. Ikeuchi, M. Matsuoka, S. Harada, H. Mitsuya, S. Kimura, and S. Oka.** 2004. Novel patterns of nevirapine resistance-associated mutations of human immunodeficiency virus type 1 in treatment-naive patients. Virology **327**:215–224.
13. **Hanna, G. J., and R. T. D'Aquila.** 2001. Clinical use of genotypic and phenotypic drug resistance testing to monitor antiretroviral chemotherapy. Clin. Infect. Dis. **32**:774–782.
14. **Hertogs, K., M. P. de Bethune, V. Miller, T. Ivens, P. Schel, A. Van Cauwenberge, C. Van Den Eynde, V. Van Gerwen, H. Azijn, M. Van Houtte, F. Peeters, S. Staszewski, M. Conant, S. Bloor, S. Kemp, B. Larder, and R. Pauwels.** 1998. A rapid method for simultaneous detection of phenotypic resistance to inhibitors of protease and reverse transcriptase in recombinant human immunodeficiency virus type 1 isolates from patients treated with antiretroviral drugs. Antimicrob. Agents Chemother. **42**:269–276.
15. **Jang, S. K., and E. Wimmer.** 1990. Cap-independent translation of encephalomyocarditis virus RNA: structural elements of the internal ribosomal entry site and involvement of a cellular 57-kD RNA-binding protein. Genes Dev. **4**:1560–1572.
16. **Jones, S., and M. E. Klotman.** 2001. Impact of genotypic resistance testing on physician selection of antiretroviral therapy. J. Hum. Virol. **4**:214–216.
17. **Kajiwara, K., E. Kodama, and M. Matsuoka.** 2006. A novel colorimetric assay for CXCR4 and CCR5 tropic human immunodeficiency viruses. Antivir. Chem. Chemother. **17**:215–223.
18. **Kellam, P., and B. A. Larder.** 1994. Recombinant virus assay: a rapid, phenotypic assay for assessment of drug susceptibility of human immunodeficiency virus type 1 isolates. Antimicrob. Agents Chemother. **38**:23–30.
19. **Ketas, T. J., S. E. Kuhmann, A. Palmer, J. Zurita, W. He, S. K. Ahuja, P. J. Klasse, and J. P. Moore.** 2007. Cell surface expression of CCR5 and other host factors influence the inhibition of HIV-1 infection of human lymphocytes by CCR5 ligands. Virology **364**:281–290.
20. **Kimpton, J., and M. Emerman.** 1992. Detection of replication-competent and pseudotyped human immunodeficiency virus with a sensitive cell line on the basis of activation of an integrated β-galactosidase gene. J. Virol. **66**: 2232–2239.
21. **Korn, K., H. Reil, H. Walter, and B. Schmidt.** 2003. Quality control trial for human immunodeficiency virus type 1 drug resistance testing using clinical samples reveals problems with detecting minority species and interpretation of test results. J. Clin. Microbiol. **41**:3559–3565.
22. **Lalezari, J. P., K. Henry, M. O'Hearn, J. S. Montaner, P. J. Piliero, B. Trottier, S. Walmsley, C. Cohen, D. R. Kuritzkes, J. J. Eron, Jr., J. Chung, R. DeMasi, L. Donatacci, C. Drobnes, J. Delehanty, and M. Salgo.** 2003. Enfuvirtide, an HIV-1 fusion inhibitor, for drug-resistant HIV infection in North and South America. N. Engl. J. Med. **348**:2175–2185.
23. **Lazzarin, A., B. Clotet, D. Cooper, J. Reynes, K. Arasteh, M. Nelson, C. Katlama, H. J. Stellbrink, J. F. Delfraissy, J. Lange, L. Huson, R. DeMasi, C. Wat, J. Delehanty, C. Drobnes, and M. Salgo.** 2003. Efficacy of enfuvirtide in patients infected with drug-resistant HIV-1 in Europe and Australia. N. Engl. J. Med. **348**:2186–2195.
24. **Loutfy, M. R., J. M. Raboud, J. S. Montaner, T. Antoniou, B. Wynhoven, F. Smaill, D. Rouleau, J. Gill, W. Schlech, Z. L. Brumme, T. Mo, K. Gough, A. Rachlis, P. R. Harrigan, and S. L. Walmsley.** 2007. Assay of HIV gp41 amino acid sequence to identify baseline variation and mutation development in patients with virologic failure on enfuvirtide. Antivir. Res. **75**:58–63.
25. **Maguire, M. F., R. Guinea, P. Griffin, S. Macmanus, R. C. Elston, J. Wolfram, N. Richards, M. H. Hanlon, D. J. Porter, T. Wrin, N. Parkin, M. Tisdale, E. Furfine, C. Petropoulos, B. W. Snowden, and J. P. Kleim.** 2002. Changes in human immunodeficiency virus type 1 Gag at positions L449 and P453 are linked to I50V protease mutants in vivo and cause reduction of sensitivity to amprenavir and improved viral fitness in vitro. J. Virol. **76**:7398–7406.
26. **Nikolenko, G. N., K. A. Delviks-Frankenberry, S. Palmer, F. Maldarelli, M. J. Fivash, Jr., J. M. Coffin, and V. K. Pathak.** 2007. Mutations in the connection domain of HIV-1 reverse transcriptase increase 3′-azido-3′-deoxythymidine resistance. Proc. Natl. Acad. Sci. USA **104**:317–322.
27. **Perez-Alvarez, L., R. Carmona, A. Ocampo, A. Asorey, C. Miralles, S. Perez de Castro, M. Pinilla, G. Contreras, J. A. Taboada, and R. Najera.** 2006. Long-term monitoring of genotypic and phenotypic resistance to T20 in treated patients infected with HIV-1. J. Med. Virol. **78**:141–147.
28. **Pion, M., A. Jordan, A. Biancotto, F. Dequiedt, F. Gondois-Rey, S. Rondeau, R. Vigne, J. Hejnar, E. Verdin, and I. Hirsch.** 2003. Transcriptional suppression of in vitro-integrated human immunodeficiency virus type 1 does not correlate with proviral DNA methylation. J. Virol. **77**:4025–4032.
29. **Reeves, J. D., S. A. Gallo, N. Ahmad, J. L. Miamidian, P. E. Harvey, M. Sharron, S. Pohlmann, J. N. Sfakianos, C. A. Derdeyn, R. Blumenthal, E. Hunter, and R. W. Doms.** 2002. Sensitivity of HIV-1 to entry inhibitors correlates with envelope/coreceptor affinity, receptor density, and fusion kinetics. Proc. Natl. Acad. Sci. USA **99**:16249–16254.
30. **Rhee, S. Y., J. Taylor, G. Wadhera, A. Ben-Hur, D. L. Brutlag, and R. W. Shafer.** 2006. Genotypic predictors of human immunodeficiency virus type 1 drug resistance. Proc. Natl. Acad. Sci. USA **103**:17355–17360.
31. **Richman, D. D.** 2000. Principles of HIV resistance testing and overview of assay performance characteristics. Antivir. Ther. **5**:27–31.
32. **Salomon, H., A. Belmonte, K. Nguyen, Z. Gu, M. Gelfand, and M. A. Wainberg.** 1994. Comparison of cord blood and peripheral blood mononuclear cells as targets for viral isolation and drug sensitivity studies involving human immunodeficiency virus type 1. J. Clin. Microbiol. **32**:2000–2002.
33. **Sarmati, L., E. Nicastri, S. G. Parisi, G. d'Ettorre, G. Mancino, P. Narciso, V. Vullo, and M. Andreoni.** 2002. Discordance between genotypic and phenotypic drug resistance profiles in human immunodeficiency virus type 1 strains isolated from peripheral blood mononuclear cells. J. Clin. Microbiol. **40**:335–340.
34. **Shafer, R. W., M. J. Kozal, D. A. Katzenstein, W. H. Lipil, I. F. Johnstone, and T. C. Merigan.** 1993. Zidovudine susceptibility testing of human immunodeficiency virus type 1 (HIV) clinical isolates. J. Virol. Methods **41**:297–310.
35. **Shi, C., and J. W. Mellors.** 1997. A recombinant retroviral system for rapid in vivo analysis of human immunodeficiency virus type 1 susceptibility to reverse transcriptase inhibitors. Antimicrob. Agents Chemother. **41**:2781–2785.
36. **Soda, Y., N. Shimizu, A. Jinno, H. Y. Liu, K. Kanbe, T. Kitamura, and H. Hoshino.** 1999. Establishment of a new system for determination of coreceptor usages of HIV based on the human glioma NP-2 cell line. Biochem. Biophys. Res. Commun. **258**:313–321.
37. **Tamamura, H., Y. Xu, T. Hattori, X. Zhang, R. Arakaki, K. Kanbara, A. Omagari, A. Otaka, T. Ibuka, N. Yamamoto, H. Nakashima, and N. Fujii.** 1998. A low-molecular-weight inhibitor against the chemokine receptor CXCR4: a strong anti-HIV peptide T140. Biochem. Biophys. Res. Commun. **253**:877–882.

Design of a Novel HIV-1 Fusion Inhibitor That Displays a Minimal Interface for Binding Affinity

Shinya Oishi,*,† Saori Ito,† Hiroki Nishikawa,† Kentaro Watanabe,† Michinori Tanaka,† Hiroaki Ohno,† Kazuki Izumi,‡ Yasuko Sakagami,‡ Eiichi Kodama,‡ Masao Matsuoka,‡ and Nobutaka Fujii*,†

Graduate School of Pharmaceutical Sciences, Kyoto University, Sakyo-ku, Kyoto 606-8501, Japan, and Laboratory of Virus Immunology, Institute for Virus Research, Kyoto University, Sakyo-ku, Kyoto 606-8507, Japan

Received September 6, 2007

Abstract: Reported herein are the design, biological activities, and biophysical properties of a novel HIV-1 membrane fusion inhibitor. α-Helix-inducible X-EE-XX-KK motifs were applied to design an enfuvirtide analogue **2** that exhibited highly potent anti-HIV activity against wild-type HIV-1, enfuvirtide-resistant HIV-1 strains, and an HIV-2 strain in vitro. Indispensable residues for bioactivity of enfuvirtide, including the residues interacting with the N-terminal heptad repeat and the C-terminal hydrophobic residues, were identified.

The viral entry process of human immunodeficiency virus type 1 (HIV-1[a]) into target cells is mediated by envelope glycoprotein gp41. Formation of a fusogenic six-helical bundle structure consisting of a gp41 N-terminal heptad repeat (NHR) and C-terminal heptad repeat (CHR) promotes the fusion of viral and cellular membranes (Figure 1a).[1] Enfuvirtide **1** (T-20, DP178) is an approved anti-HIV peptide derived from the gp41 CHR.[2,3] This first drug that inhibits HIV-1 entry into the cell is utilized as an alternative anti-HIV agent for patients with drug resistance to reverse transcriptase and/or protease inhibitors. It is believed that peptide **1** interacts with the NHR of gp41 prehairpin structure[4] and associates with the cell or viral membrane through a C-terminal tryptophan-rich region,[5–7] but the exact action mechanism of **1** has not been clarified.[8,9]

Stabilization of bioactive conformations of peptides is a promising approach to enhance their biological potency and to understand the bioactive conformation. Several approaches to stabilize the α-helix structure of gp41 CHR have been reported including macrocyclization by covalent bond formation[10] or salt-bridge formation[11–13] between two adjacent residues and/or introduction of α-helix-inducible peptide sequences.[11] The analogue of another CHR peptide C34, in which the residues on the outer surface of the six-helical bundle were comprehensively replaced with glutamates (Glu) or lysines (Lys), retained highly potent anti-HIV activity.[12] This indicates that the substituted residues are not associated with an NHR coiled-coil as suggested by the crystal structure of the N36-C34 complex.[14] Our expectation was that the following three functional surfaces of **1** could be characterized by extending this molecular design (Figure 1b): (1) minimal interface residues for affinity with NHR; (2) solvent-accessible sites to be utilized for α-helix inducible salt bridges; (3) another functional region outside the α-helix structure. Accordingly, efforts herein were undertaken to design novel amphiphilic enfuvirtide derivatives bearing α-helix-inducible motifs.

A schematic wheel of the potential α-helix structure of peptide **1** is depicted in Figure 1c. To introduce salt bridges between i and $i + 4$ residues on the basis of the previous C34 modification,[12] Glu and Lys were arranged at b/c and f/g positions, respectively, so that four consecutive X-EE-XX-KK motifs appeared in the designed peptide **2** (designated T-20EK, Figure 2). All peptides were prepared by standard Fmoc-based peptide synthesis protocol. After final deprotection and cleavage from the resins using a TFA/thioanisole/*m*-cresol/ethanedithiol/H_2O (80:5:5:5:5) cocktail, the crude peptides were purified by reverse-phase HPLC to yield the expected peptides, which were characterized by mass spectrometry. Anti-HIV activity of the peptides against laboratory HIV-1 NL4-3 strain (wild-type) was evaluated by MAGI assay (Table 1). Peptide **2** exhibited 8-fold greater anti-HIV activity compared with the parent peptide **1** [peptide **1**, $EC_{50} = 15 \pm 3.9$ nM; peptide **2**, $EC_{50} = 1.8 \pm 0.4$ nM].[15] The circular dichroism (CD) spectrum of **2** in phosphate buffered saline (pH 7.4) had negative minima at 208 and 222 nm, indicating the presence of an α-helical conformation, while that of **1** suggested a random-coil conformation (Figure 3a). The significant increase in anti-HIV activity of **2** could be rationalized by the preordered stable α-helical structure upstream of L158.[16]

Systematic substitutions of the amino acids at the b, c, f, and g positions with Glu or Lys were extended (Figure 2). Peptide **3**, in which L130 and N160 were substituted with Lys and Glu, respectively, showed anti-HIV activity similar to that of peptide **2** (peptide **3**, $EC_{50} = 2.8 \pm 0.6$ nM). This is consistent with the fact that potent T-1249 also contains these two substitutions.[17] Further replacement toward the N-terminal f position (S129) was again permissive of the high anti-HIV activity (peptide **4**, $EC_{50} = 2.5 \pm 0.6$ nM). On the other hand, replacement of W161 with Glu resulted in a significant decrease of anti-HIV activity as observed in peptides **5** and **6** (EC_{50} = 185 and 111 nM, respectively), indicating that W161 may be located outside the amphiphilic α-helical region. This result correlates with the reduced entry ability of W161F mutant virus.[18] Alanine substitution of W161 also supports the relevance of this residue in virus infectivity and in the inhibitory activity of **1**. Although peptide **7**, carrying a W155A substitution, expressed anti-HIV activity similar to that of peptide **2** (peptide **7**, $EC_{50} = 5.8 \pm 1.0$ nM), W159A, W161A, and F162A substitutions showed reduced bioactivity (peptides **8**, **9**, and **10**, EC_{50} = 49, 24, and 27 nM, respectively). The observed similar CD spectra among peptides **2** and **7**–**10** demonstrated that alanine substitution had no effect on the stabilized secondary structure of the α-helix (Figure 3b). That is, the hydrophobic indole and phenyl groups of these peptides may contribute to their direct interaction with virus components such as gp41 NHR or the virus membrane.[19]

The comparative binding affinity of peptides **1** and **2** with the gp41 NHR sequence was investigated by pull-down assay using synthetic His-tagged CHR peptides and recombinant MBP-fused NHR protein (Figure 4a). Peptide **2** showed higher affinity with NHR compared with **1**. In contrast, only weak binding was observed in the same experiment using all-D-T-20EK D-**2**, which consists of all D-amino acids, indicating that

* To whom correspondence should be addressed. Phone: +81-75-753-4551. Fax: +81-75-753-4570. E-mail: for S.O., soishi@pharm.kyoto-u.ac.jp; for N.F., nfujii@pharm.kyoto-u.ac.jp.

† Graduate School of Pharmaceutical Sciences.

‡ Institute for Virus Research.

[a] Abbreviations: HIV-1, human immunodeficiency virus type 1; NHR, N-terminal heptad repeat; CHR, C-terminal heptad repeat.

10.1021/jm701109d CCC: $40.75
Published on Web 01/16/2008

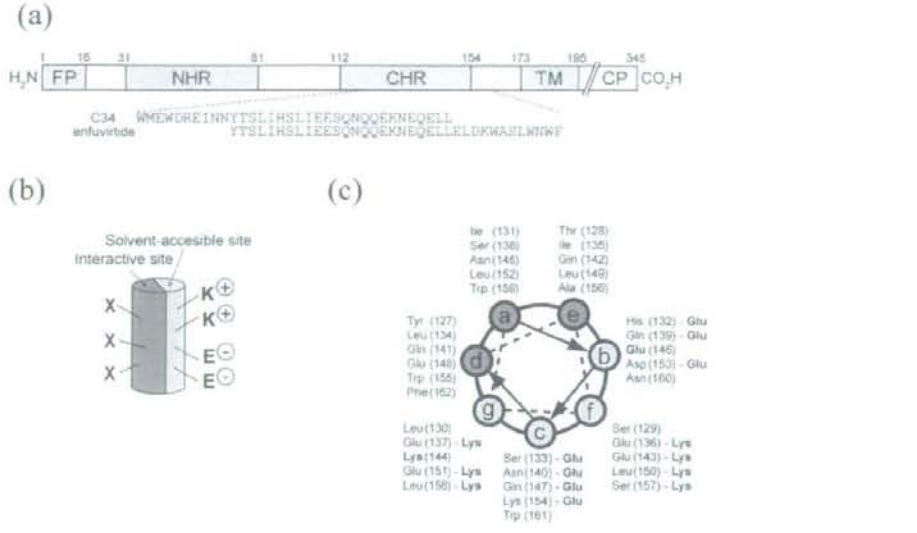

Figure 1. Design of enfuvirtide analogues: (a) schematic representation of HIV-1 gp41 (FP, fusion peptide; NHR, N-terminal heptad repeat; CHR, C-terminal heptad repeat; TM, transmembrane domain); (b) estimated preordered α-helix structure of CHR peptide by potential salt-bridge formation; (c) helical-wheel representation of peptides **1** and **2**. For peptide **2**, Glu residues are in b and e positions and Lys residues in f and g positions. Residues are numbered starting at the first amino acid of the NL4-3 gp41.

Ac-YTSLIHSLIEESQNQQEKNEQELLELDKWASLWNWF-$CONH_2$	**1** (enfuvirtide)
Ac------**EE**--**KK**-**EE**--K---E--**KK**-**EE**--**KK**-----$CONH_2$	**2**
Ac----K-**EE**--**KK**-**EE**--K---E--**KK**-**EE**--**KK**-E---$CONH_2$	**3**
Ac---KK-**EE**--**KK**-**EE**--K---E--**KK**-**EE**--**KK**-E---$CONH_2$	**4**
Ac----K-**EE**--**KK**-**EE**--K---E--**KK**-**EE**--**KK**-EE--$CONH_2$	**5**
Ac---KK-**EE**--**KK**-**EE**--K---E--**KK**-**EE**--**KK**-EE--$CONH_2$	**6**
Ac------**EE**--**KK**-**EE**--K---E--**KK**-**EE**A-**KK**-----$CONH_2$	**7**
Ac------**EE**--**KK**-**EE**--K---E--**KK**-**EE**--**KK**A----$CONH_2$	**8**
Ac------**EE**--**KK**-**EE**--K---E--**KK**-**EE**--**KK**--A--$CONH_2$	**9**
Ac------**EE**--**KK**-**EE**--K---E--**KK**-**EE**--**KK**---A-$CONH_2$	**10**
Ac-LDAN-TK-L--A-I-----MY--QK-NQ-DIFS----$CONH_2$	**11**
Ac-WQEWEQK-TA-L-QA-I------Y--QK--------E---$CONH_2$	T-1249

Figure 2. Peptide sequences of enfuvirtide, enfuvirtide analogues, and T-1249.

Table 1. Anti-HIV Activity of Synthetic Enfuvirtide Analogues

peptide	EC_{50} (nM)[a]	peptide	EC_{50} (nM)[a]
1 (enfuvirtide)	15 ± 3.9	**7**	5.8 ± 1.0
2[b]	1.8 ± 0.4	**8**	49 ± 8.6
3	2.8 ± 0.6	**9**	24 ± 3.8
4	2.5 ± 0.6	**10**	27 ± 6.8
5	185 ± 17	C34	4.5 ± 0.5
6	111 ± 25		

[a] EC_{50} was determined as the concentration that blocked HIV-1 replication by 50% in MAGI assay. [b] The enantiomer of peptide **2** (D-**2**) did not show anti-HIV activity at 10 μM.

the binding between **2** and NHR is specific. In addition, peptide **2** inhibited the interaction between **1** and NHR in lower concentration in the inhibition experiment (Figure 4b).[20]

We next evaluated the anti-HIV activity of peptide **2** against enfuvirtide-resistant variants HIV-1_{V38A} and HIV-1_{N43D}, which were mainly isolated from patients resistant to enfuvirtide (Table 2).[21] Because of the deficient replication of these variants,[22] an additional D36G mutation was experimentally added to these variants and to the wild-type virus. The D36G mutation is not involved in enfuvirtide resistance, but it did improve the sensitivity against **1** [EC_{50}(HIV-1_{D36G}) = 2.3 nM] compared with wild-type HIV-1. As reported previously,[21] V38A and N43D mutations significantly reduced the potency of **1** [EC_{50} (HIV-1_{V38A}) = 22 nM; EC_{50}(HIV-1_{N43D}) = 46 nM]. On the other hand, peptide **2** retained similar anti-HIV activity against N43D and slightly less potent activity toward V38A variants [EC_{50}(HIV-1_{V38A}) = 3.3 nM; EC_{50}(HIV-1_{N43D}) = 1.7 nM]. It is of interest that the anti-HIV activity was restored by induction of a bioactive α-helix structure using X-EE-XX-KK motifs on a CHR peptide. This implies that the stable α-helical structure of **2** can overcome the reduced affinity derived from the mismatched interaction between mutated NHR sequences and peptide **1**.

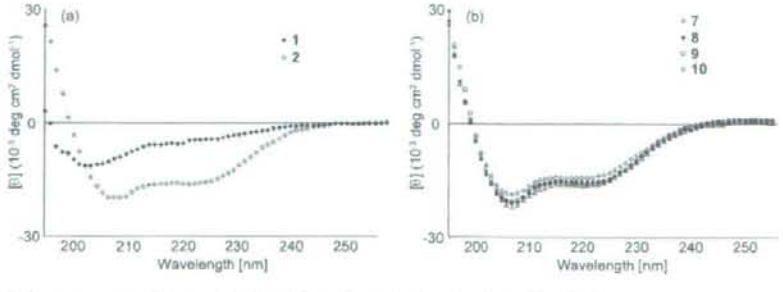

Figure 3. Circular dichroism spectra of (a) peptides **1** and **2** and (b) Ala-substituted peptides **7**–**10**.

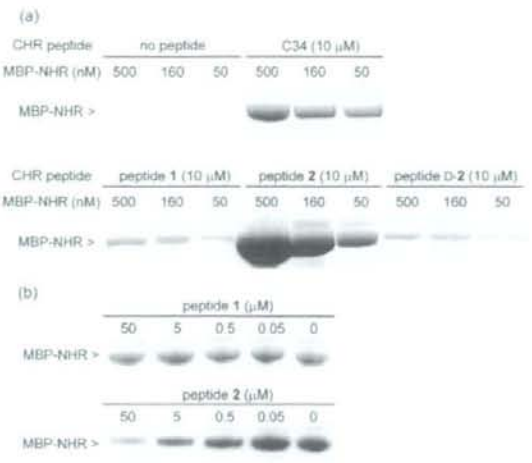

Figure 4. Interaction of His-tagged CHR peptides with MBP-NHR protein by pull-down assay and SDS−PAGE: (a) NHR protein binding with several His-tagged CHR peptides; (b) inhibition of interaction between His-tagged enfuvirtide and NHR protein by nontagged peptides **1** and **2**.

Table 2. Anti-HIV Activity of Peptides **1** and **2** against Enfuvirtide-Resistant Variant and HIV-2 Strains

	EC_{50} (nM)[a]	
strains	peptide **1**	peptide **2**
HIV-1		
NL4–3	15 ± 3.9	1.8 ± 0.4
D36G	2.3 ± 0.5	0.9 ± 0.2
D36G V38A	22 ± 7.6	3.3 ± 1.0
D36G N43D	46 ± 9.6	1.7 ± 0.3
HIV-2		
EHO[b]	37 ± 10	1.5 ± 0.5

[a] EC_{50} was determined as the concentration that blocked HIV-1 replication by 50% in MAGI assay. [b] The antiviral activity (EC_{50}) of peptide **11** against EHO strain was 2.1 ± 0.7 nM.

Interestingly, peptide **2** showed potent antiviral activity even against an HIV-2 EHO strain [EC_{50} = 1.5 nM], which is as potent as peptide **11** having a congenerous sequence derived from the EHO strain [EC_{50} = 2.1 nM].[23] This is in contrast to the previous report on the reduced activity of **1** against the EHO strain [EC_{50} = 37 nM].[24] The potent bioactivity of **2** can be rationalized by the minimal difference of the interface residues between HIV-1 and -2 and the stabilized α-helix structure. Among 19 different residues between the sequences of NL4-3 and EHO strains, 13 residues are located at the solvent accessible sites (b, c, f, and g positions). Although the other six residues are possibly involved in the direct interaction, the potential reduced interactions derived from the mismatch could be recovered by introduction of X-EE-XX-KK motifs.

In conclusion, remodeling of **1** to yield the preordered α-helical structure of **2** led to improved affinity with NHR and increased antiviral activity even against enfuvirtide-resistant HIV-1 and HIV-2 strains. This approach also helped to clarify the potential minimal interface of **1** with viral gp41. Peptide **2** could be a useful chemical tool to understand the membrane fusion process of HIV-1 and the detailed action mechanism of enfuvirtide.

Acknowledgment. This work was supported by a Grant-in-Aid for Scientific Research from the Ministry of Education, Culture, Sports, Science, and Technology of Japan, Health and Labour Sciences Research Grants (Research on HIV/AIDS), the 21st Century COE Program's "Knowledge Information Infrastructure for Genome Science", and the Japan Science and Technology Agency. H.N. is grateful for the JSPS Research Fellowships for Young Scientists. Appreciation is expressed to Dr. Masaru Hoshino (Kyoto University) for helpful discussions and to Mr. Maxwell Reback (Kyoto University) for reading the manuscript.

Supporting Information Available: Experimental details for peptide preparation, CD spectra measurements, and bioassays and MS and HPLC data. This material is available free of charge via the Internet at http://pubs.acs.org.

References

(1) Lu, M.; Blacklow, S. C.; Kim, P. S. A trimeric structural domain of the HIV-1 transmembrane glycoprotein. *Nat. Struct. Biol.* **1995**, *2*, 1075–1082.
(2) Wild, C. T.; Shugars, D. C.; Greenwell, T. K.; McDanal, C. B.; Matthews, T. J. Peptides corresponding to a predictive alpha-helical domain of human immunodeficiency virus type 1 gp41 are potent inhibitors of virus infection. *Proc. Natl. Acad. Sci. U.S.A.* **1994**, *91*, 9770–9774.
(3) Matthews, T.; Salgo, M.; Greenberg, M.; Chung, J.; DeMasi, R.; Bolognesi, D. Enfuvirtide: the first therapy to inhibit the entry of HIV-1 into host CD4 lymphocytes. *Nat. Rev. Drug. Discovery* **2004**, *3*, 215–225.
(4) Lawless, M. K.; Barney, S.; Guthrie, K. I.; Bucy, T. B.; Petteway, S. R., Jr.; Merutka, G. HIV-1 membrane fusion mechanism: structural studies of the interactions between biologically-active peptides from gp41. *Biochemistry* **1996**, *35*, 13697–13708.
(5) Kliger, Y.; Gallo, S. A.; Peisajovich, S. G.; Munoz-Barroso, I.; Avkin, S.; Blumenthal, R.; Shai, Y. Mode of action of an antiviral peptide from HIV-1. Inhibition at a post-lipid mixing stage. *J. Biol. Chem.* **2001**, *276*, 1391–1397.
(6) Cardoso, R. M.; Zwick, M. B.; Stanfield, R. L.; Kunert, R.; Binley, J. M.; Katinger, H.; Burton, D. R.; Wilson, I. A. Broadly neutralizing anti-HIV antibody 4E10 recognizes a helical conformation of a highly conserved fusion-associated motif in gp41. *Immunity* **2005**, *22*, 163–173.
(7) Wexler-Cohen, Y.; Johnson, B. T.; Puri, A.; Blumenthal, R.; Shai, Y. Structurally altered peptides reveal an important role for N-terminal heptad repeat binding and stability in the inhibitory action of HIV-1 peptide DP178. *J. Biol. Chem.* **2006**, *281*, 9005–9010.
(8) Liu, S.; Lu, H.; Niu, J.; Xu, Y.; Wu, S.; Jiang, S. Different from the HIV fusion inhibitor C34, the anti-HIV drug Fuzeon (T-20) inhibits HIV-1 entry by targeting multiple sites in gp41 and gp120. *J. Biol. Chem.* **2005**, *280*, 11259–11273.
(9) Liu, S.; Jing, W.; Cheung, B.; Lu, H.; Sun, J.; Yan, X.; Niu, J.; Farmar, J.; Wu, S.; Jiang, S. HIV gp41 C-terminal heptad repeat contains multifunctional domains. Relation to mechanisms of action of anti-HIV peptides. *J. Biol. Chem.* **2007**, *282*, 9612–9620.
(10) Judice, J. K.; Tom, J. Y.; Huang, W.; Wrin, T.; Vennari, J.; Petropoulos, C. J.; McDowell, R. S. Inhibition of HIV type 1 infectivity by constrained α-helical peptides: implications for the viral fusion mechanism. *Proc. Natl. Acad. Sci. U.S.A.* **1997**, *94*, 13426–13430.
(11) Joyce, J. G.; Hurni, W. M.; Bogusky, M. J.; Garsky, V. M.; Liang, X.; Citron, M. P.; Danzeisen, R. C.; Miller, M. D.; Shiver, J. W.; Keller, P. M. Enhancement of α-helicity in the HIV-1 inhibitory peptide DP178 leads to an increased affinity for human monoclonal antibody 2F5 but does not elicit neutralizing responses in vitro. *J. Biol. Chem.* **2002**, *277*, 45811–45820.
(12) Otaka, A.; Nakamura, M.; Nameki, D.; Kodama, E.; Uchiyama, S.; Nakamura, S.; Nakano, H.; Tamamura, H.; Kobayashi, Y.; Matsuoka, M.; Fujii, N. Remodeling of gp41-C34 peptide leads to highly effective inhibitors of the fusion of HIV-1 with target cells. *Angew. Chem., Int. Ed.* **2002**, *41*, 2937–2940.
(13) Dwyer, J. J.; Wilson, K. L.; Davison, D. K.; Freel, S. A.; Seedorff, J. E.; Wring, S. A.; Tvermoes, N. A.; Matthews, T. J.; Greenberg, M. L.; Delmedico, M. K. Design of helical, oligomeric HIV-1 fusion inhibitor peptides with potent activity against enfuvirtide-resistant virus. *Proc. Natl. Acad. Sci. U.S.A.* **2007**, *104*, 12772–12777.
(14) Chan, D. C.; Fass, D.; Berger, J. M.; Kim, P. S. Core structure of gp41 from the HIV envelope glycoprotein. *Cell* **1997**, *89*, 263–273.
(15) Cytotoxicity of peptide **2** was not observed even at 10 μM.
(16) Additional effects on increasing the anti-HIV activity such as formation of intra- and intermolecular salt bridges are also possible.
(17) Eron, J. J.; Gulick, R. M.; Bartlett, J. A.; Merigan, T.; Arduino, R.; Kilby, J. M.; Yangco, B.; Diers, A.; Drobnes, C.; DeMasi, R.;

Greenberg, M.; Melby, T.; Raskino, C.; Rusnak, P.; Zhang, Y.; Spence, R.; Miralles, G. D. Short-term safety and antiretroviral activity of T-1249, a second-generation fusion inhibitor of HIV. *J. Infect. Dis.* **2004**, *189*, 1075–1083.

(18) Salzwedel, K.; West, J. T.; Hunter, E. A conserved tryptophan-rich motif in the membrane-proximal region of the human immunodeficiency virus type 1 gp41 ectodomain is important for Env-mediated fusion and virus infectivity. *J. Virol.* **1999**, *73*, 2469–2480.

(19) Wexler-Cohen, Y.; Johnson, B. T.; Puri, A.; Blumenthal, R.; Shai, Y. Structurally altered peptides reveal an important role for N-terminal heptad repeat binding and stability in the inhibitory action of HIV-1 peptide DP178. *J. Biol. Chem.* **2006**, *281*, 9005–9010.

(20) Since a large excess of CHR peptides to NHR protein was utilized for the pull-down assay, the inhibitory concentration in this experiment was less than that observed in the MAGI assay. It is conceivable that the anti-HIV activity in the MAGI assay might be observed with less fully occupied one or two CHR peptides bound per NHR trimer.

(21) Cabrera, C.; Marfil, S.; Garcia, E.; Martinez-Picado, J.; Bonjoch, A.; Bofill, M.; Moreno, S.; Ribera, E.; Domingo, P.; Clotet, B.; Ruiz, L. Genetic evolution of gp41 reveals a highly exclusive relationship between codons 36, 38 and 43 in gp41 under long-term enfuvirtide-containing salvage regimen. *AIDS* **2006**, *20*, 2075–2080.

(22) Mink, M.; Mosier, S. M.; Janumpalli, S.; Davison, D.; Jin, L.; Melby, T.; Sista, P.; Erickson, J.; Lambert, D.; Stanfield-Oakley, S. A.; Salgo, M.; Cammack, N.; Matthews, T.; Greenberg, M. L. Impact of human immunodeficiency virus type 1 gp41 amino acid substitutions selected during enfuvirtide treatment on gp41 binding and antiviral potency of enfuvirtide in vitro. *J. Virol.* **2005**, *79*, 12447–12454.

(23) Gustchina, E.; Hummer, G.; Bewley, C. A.; Clore, G. M. Differential inhibition of HIV-1 and SIV envelope-mediated cell fusion by C34 peptides derived from the C-terminal heptad repeat of gp41 from diverse strains of HIV-1, HIV-2, and SIV. *J. Med. Chem.* **2005**, *48*, 3036–3044.

(24) Witvrouw, M.; Pannecouque, C.; Switzer, W. M.; Folks, T. M.; De Clercq, E.; Heneine, W. Susceptibility of HIV-2, SIV and SHIV to various anti-HIV-1 compounds: implications for treatment and post-texposure prophylaxis. *Antiviral Ther.* **2004**, *9*, 57–65.

JM701109D

JOURNAL OF VIROLOGY, Jan. 2008, p. 588–592 Vol. 82, No. 1
0022-538X/08/$08.00+0 doi:10.1128/JVI.01697-07

Heptad Repeat-Derived Peptides Block Protease-Mediated Direct Entry from the Cell Surface of Severe Acute Respiratory Syndrome Coronavirus but Not Entry via the Endosomal Pathway▽

Makoto Ujike,[1]† Hiroki Nishikawa,[2]† Akira Otaka,[3] Naoki Yamamoto,[4] Norio Yamamoto,[4] Masao Matsuoka,[5] Eiichi Kodama,[5] Nobutaka Fujii,[2,5]* and Fumihiro Taguchi[1]*

Department of Virology III, National Institute of Infectious Disease, Gakuen 4-7-1, Musashi-murayama, Tokyo 208-0011, Japan[1]; Graduate School of Pharmaceutical Sciences, Kyoto University, Sakyo-ku, Kyoto 606-8501, Japan[2]; Graduate School of Pharmaceutical Sciences, The University of Tokushima, Tokushima 770-8505, Japan[3]; Department of Molecular Virology, Tokyo Medical and Dental University, 1-5-45 Yushima, Bunkyo-ku, Tokyo 113-8519, Japan[4]; and Institute for Virus Research, Kyoto University, Sakyo-ku, Kyoto 606-8507, Japan[5]

Received 6 August 2007/Accepted 6 October 2007

The peptides derived from the heptad repeat (HRP) of severe acute respiratory syndrome coronavirus (SCoV) spike protein (sHRPs) are known to inhibit SCoV infection, yet their efficacies are fairly low. Recently our research showed that some proteases facilitated SCoV's direct entry from the cell surface, resulting in a more efficient infection than the previously known infection via endosomal entry. To compare the inhibitory effect of the sHRP in each pathway, we selected two sHRPs, which showed a strong inhibitory effect on the interaction of two heptad repeats in a rapid and virus-free in vitro assay system. We found that they efficiently inhibited SCoV infection of the protease-mediated cell surface pathway but had little effect on the endosomal pathway. This finding suggests that sHRPs may effectively prevent infection in the lungs, where SCoV infection could be enhanced by proteases produced in this organ. This is the first observation that HRP exhibits different effects on virus that takes the endosomal pathway and virus that enters directly from the cell surface.

Severe acute respiratory syndrome (SARS) coronavirus (SCoV) is a causative agent of life-threatening SARS (4, 7, 15, 31). Although the first outbreak of SARS was stamped out, an effective antiviral drug is still required for the treatment and prevention of possible future outbreaks. SCoV is an enveloped virus and enters cells via fusion between the cellular membrane and its envelope. SCoV membrane fusion is mediated by the spike (S) protein, which is classified as a class I fusion protein. One of the most important features of class I fusion proteins is the conserved heptad repeat regions (HR1 and HR2) which play an essential role in virus-cell fusion activities (3, 6, 10, 28). In the fusion process, HR1 forms an interior, trimeric coiled-coil structure to which HR2 binds in an antiparallel fashion, resulting in the formation of a six-helix bundle. This structure brings viral and cellular membranes into close proximity to facilitate membrane fusion. Synthetic short peptides derived from the HR (HRP) of class I fusion proteins have been shown to block the interaction of HR1-HR2 complexes, resulting in the inhibition of a number of viral infections, including those of retroviruses (11, 14, 21, 23, 32, 38, 39), paramyxoviruses (12, 16, 30, 36, 42–44), filovirus (37), and coronavirus (2). Similarly, HRP of SCoV S (sHRP) could also inhibit SCoV and human immunodeficiency virus (HIV)/SCoV-pseudotyped virus infection (1, 18, 24, 45). However, these inhibitory effects were significantly less than those of one of the most effective HRPs from HIV type 1 (HIV-1) (39) and even those from the same family, murine coronavirus mouse hepatitis virus (MHV) (2).

The major organs targeted by SCoV are the lungs and intestines, although the virus grows in a variety of tissues that express angiotensin-converting enzyme 2 (ACE2). Recently we and others showed that SCoV uses two distinct entry pathways depending on the presence of proteases (20, 33, 34). In the absence of proteases, SCoV enters the cell via an endosomal pathway (9, 26, 41), with the S protein activated for fusion by the cathepsin L protease, which is active only under acidic conditions in the endosome (8, 33). In contrast, in the presence of protease, SCoV virion S proteins attach to ACE2 on the host cell surface and are activated for fusion by proteases such as trypsin or elastase, which leads to envelope-plasma membrane fusion and direct entry from the cell surface (20, 33, 34). Infection via the cell surface is more than 100 times more efficient than infection via the endosomal pathway (20). These results suggested the possibility that the severe illnesses in the lung and intestine could be due to the enhancement of direct SCoV cell surface entry mediated by proteases produced in these organs (20).

Although previous studies have described the inhibitory effects of the sHRP on SCoV infection via the endosomal path-

* Corresponding author. Mailing address for F. Taguchi: Department of Virology III, National Institute of Infectious Disease, Gakuen 4-7-1, Musashi-murayama, Tokyo 208-0011, Japan. Phone: 81-42-561-0771, ext. 533. Fax: 81-42-567-5631. E-mail: ftaguchi@nih.go.jp. Mailing address for N. Fujii: Graduate School of Pharmaceutical Sciences, Kyoto University, Sakyo-ku, Kyoto 606-8501, Japan. Phone: 81-75-753-4511. Fax: 81-75-753-4570. E-mail: nfujii@pharm.kyoto-u.ac.jp.

† M.U. and H.N. contributed equally to this work.

▽ Published ahead of print on 17 October 2007.

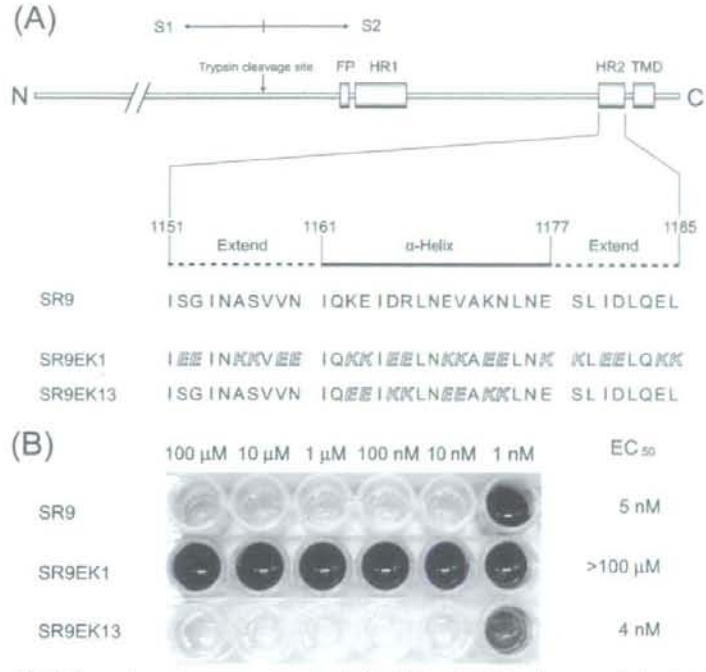

FIG. 1. (A) Schematic of SCoV S protein and sequences of native sHRP (SR9) and its EK substitution derivatives. The S protein contains two α-helical heptad repeats (HR1 and HR2), a putative fusion peptide (FP), a transmembrane domain (TMD), and a trypsin cleavage site (17). The expanded region shows the amino acid sequence of HR2 (SR9), which consists of two extended parts (1151 to 1160 and 1178 to 1185) and one α-helix part (1161 to 1177). Substituted EKs are shown with italic white letters. (B) In vitro binding inhibition assay of HRPs. GST-HR2-coated plates were incubated with MBP-HR1 in the presence of various concentrations (1 nM to 100 μM) of sHRP. Inhibitory potency of the peptide was assessed using the anti-MBP antibody-alkaline phosphatase conjugate and staining with 5-bromo-4-chloro-3-indolylphosphate.

way (1, 18, 24, 45), little is known about their effects on the protease-mediated cell surface pathway. Thus, in this study, we reevaluated the inhibitory effects of the sHRP on infection via the two distinct pathways of SCoV entry.

Recent studies of the X-ray crystal structure of the SCoV S HR1-HR2 complex have shown that the HR2 peptide consists of two extended regions and one α-helical region (35, 40). Since we have found that HRPs with replacement by the X-EE-XX-KK sequence in the HIV-1 HR2 region exhibited potent anti-HIV-1 activity (27), we chose to modify the α-helical region of HRP derived from SCoV S HR2 (sHRP) and also to prepare the control peptide SR9EK1 without sequence relatedness (Fig. 1A). To estimate these sHRPs, we established a rapid and virus-free in vitro novel assay system based on the inhibition of HR1-HR2 complex formation. Two fusion proteins (maltose binding protein [MBP]-HR1 [amino acid residues of the S protein, 892 to 964] and glutathione *S*-transferase [GST]-HR2 [1141 to 1192]) were expressed using *Escherichia coli* and purified using amylose resin (New England Biolabs) and glutathione Sepharose 4B (GE Healthcare, Bucks, United Kingdom), respectively. An enzyme-linked immunosorbent assay plate was coated with GST-HR2 dissolved in sodium carbonate buffer (pH 8.5), 3.6 μg/ml in concentration, by incubation at 4°C for 8 h. After bovine serum albumin blocking (1 mg/ml) at 4°C for 2.5 h, GST-HR2 on the plate was allowed to bind the MBP-HR1 protein (8.8 μg/ml) by incubation at 37°C for 1.5 h in the presence of various concentrations of sHRPs to be examined for inhibition activity. After the plate was washed, the inhibiting potency of the peptide was assessed by colorimetric analyses using the anti-MBP antibody-alkaline phosphatase conjugate (Sigma) with a 1:1,000 dilution with incubation at 4°C for 1 h and then staining with BluePhos microwell phosphatase (KPL). As shown in Fig. 1B, SR9 and SR9EK13 showed significant binding inhibition in a nanomolar range, whereas the control, SR9EK1, without sequence relatedness, had no inhibitory effect at a concentration of 100 μM.

We tested the inhibitory effects of SR9 and SR9EK13 on SCoV entry, since these sHRPs were found to have a strong binding inhibition activity, along with the control peptide SR9EK1. We examined their effects on both the endosomal and protease-mediated cell surface entry processes. Viral entry via the endosome was examined as described previously with a slight modification (20). In brief, VeroE6 cells were pretreated with each sHRP at 37°C for 30 min and then inoculated with SCoV (multiplicity of infection = 1.0) and incubated on ice for 30 min to allow viral attachment to ACE2 but not viral entry. After removal of unattached viruses, the cells were incubated at 37°C for 6 h. Viral entry was measured by quantifying the newly synthesized mRNA9 using real-time PCR (20). To evaluate entry via the cell surface, the cells were pretreated with 1

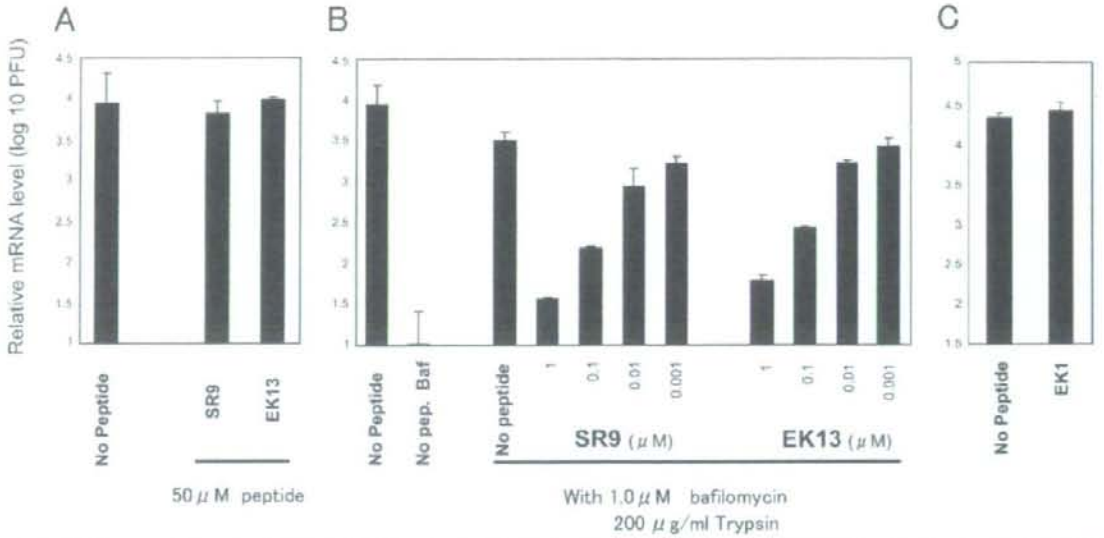

FIG. 2. Inhibitory effect of sHRPs on SCoV infections via the endosomal pathway (A) or protease-mediated cell-surface pathway (B). (A) VeroE6 cells were pretreated with 50 μM sHRPs at 37°C for 30 min, placed on ice for 10 min, and then inoculated with SCoV at a multiplicity of infection of 1.0 on ice for 30 min. After the removal of unbound virus, the cells were incubated in medium containing 50 μM sHRPs at 37°C for 6 h. (B) Cells pretreated with 1 μM Baf and sHRPs at the indicated concentrations were inoculated with SCoV as described above. After the removal of unbound virus, the cells were treated with 200 μg/ml L-1-tosylamide-2-phenylethyl chloromethyl ketone-treated trypsin at room temperature for 5 min and incubated at 37°C for 6 h. sHRP and Baf were present in the media in all steps at indicated concentrations. To measure amounts of viruses that entered cells, cells were infected with 10-fold-stepwise-diluted SARS-CoV from 10^6 to 10^2 PFU without Baf and trypsin and the amounts of mRNA9 were quantified by real-time PCR. Amounts of viral entry in this study were calculated from a calibration line obtained as described above and are shown as relative mRNA levels (20). (C) EK1 has no sequential similarity to sHRP and showed no inhibitory effect in vitro. Cells were treated with 1 μM EK1 as a control peptide, and other procedures were performed as described for panel B.

μM bafilomycin (Baf), which blocks SCoV endosomal entry, at 37°C for 30 min before SCoV inoculation. After removal of unattached viruses, the cells were treated with trypsin (0.2 mg/ml) for 5 min at room temperature and viral entry was measured as described above. Each sHRP and/or Baf was present in the media in all steps at various concentrations. In the absence of proteases, these sHRPs showed no measurable inhibitory effect on SCoV endosomal infection even at concentrations as high as 50 μM, despite showing a potent inhibitory effect in vitro (Fig. 2A). This lack of inhibition is consistent with previous observations that the same or homologous-sequence sHRPs had no inhibitory effect on SCoV infection at high concentrations of 10 μM (45) or 50 μM (1), respectively. In contrast, when SCoV was allowed to enter cells via the cell surface by treatment with protease and Baf, these sHRPs showed a strong inhibitory effect on SCoV infection in a dose-dependent manner (Fig. 2B). At a concentration of 0.1 μM, the SR9 sHRP reduced newly synthesized mRNA9 levels by about 10-fold, while an sHRP concentration of 1 μM saw a 50-fold decrease. The control sHRP, SR9EK1, did not inhibit SCoV cell-surface-mediated infection even at the concentration of 1 μM, indicating that the inhibition is peptide sequence specific (Fig. 2C). We finally evaluated the inhibitory effect of sHRPs in the presence of trypsin but without Baf treatment. These conditions may resemble the situation of patients with severe SARS, in which some proteases were produced in the infected lung and intestinal tissue. Under these conditions, these sHRPs also showed a potent inhibitory effect on SCoV infection (Fig. 3).

The present study indicates that our sHRPs fail to inhibit endosome-mediated SCoV infection. This finding is consistent with those of previous studies indicating that sHRPs have a low inhibitory effect on endosomal infection of native SCoV. The reported 50% effective dose (EC_{50}) was 3.68 to 19.0 μM (1, 18, 45). However, our results suggest that sHRPs, which showed no measurable inhibitory effect on SCoV endosomal infection, have a very strong inhibitory effect on protease-mediated cell surface SCoV infection; the EC_{50} was less than 100 nM (Fig. 2B and 3). Cell surface infection of SCoV is anticipated to occur in the lungs of SARS patients, since various types of inflammatory cells infiltrate the lung of the patients (25), and thus elastase, a protease produced in lung inflammation (13) and shown to enhance SCoV infection in cultured cells (20), could enhance SCoV infection in the lung by facilitating the infection from cell surface. Inhibitory effects of sHRPs on cell surface infection may help prevent severe damage by SCoV infection in the major target organ. Thus, the sHRPs shown in this study would be effective anti-SARS therapeutic drugs.

A few possibilities are conceivable for the explanation of an inefficient inhibitory effect of sHRPs in infection via the endosomal pathway. One is the failure of sHRPs to be trafficked to the endosome vehicles from culture medium. Thus, their concentration in the endosome is not sufficient to prevent SCoV infection. Alternatively, sHRPs may be sufficiently transported

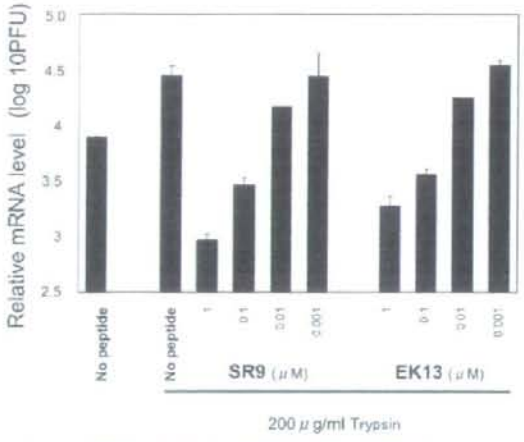

FIG. 3. Effective inhibition by HRPs of SCoV infection in the presence of exogenous trypsin. VeroE6 cells pretreated with sHRPs at the indicated concentrations were inoculated with SCoV as described in the legend to Fig. 2. After the removal of unbound virus, the cells were treated with 200 μg/ml L-1-tosylamide-2-phenylethyl chloromethyl ketone-treated trypsin at room temperature for 5 min and incubated at 37°C for 6 h. sHRPs were present in the media in all steps at the indicated concentrations. The relative viral mRNA9 was measured quantitatively by real-time PCR as described in the legend to Fig. 2. In this assay, cells were not treated with Baf throughout the experiment.

to the endosome but are inactivated by the low-pH environment or are degraded or digested with proteases present in the endosome. Another possibility is that the conformation of the cleaved S protein in the acidic environment of the endosome is different from that in a neutral pH and the sHRP fails to bind to the S protein in the former environment even if six-helix bundles with intramolecular HR2 are formed under both conditions. We are currently studying whether the inefficient inhibition of virus entry into cells could be attributed to one of those possibilities, or even another.

Interestingly, the EC_{50} (approximately 680 μM) of HRP of Ebola virus (37), which is thought to enter cells via an endosomal pathway, is remarkably higher than those of other viruses which enter cells directly from the cell surface. The inhibition with HRP of influenza virus infection, which also uses an endosomal pathway, has not yet been reported, even though its hemagglutinin protein is the prototype class I fusion protein and its cell entry mechanism has been extensively studied. In contrast, HRP of avian leucosis sarcoma virus, which uses the endosomal pathway, was reported to inhibit the infection fairly efficiently (EC_{50} = 25 to 170 nM) (5, 23). The inhibition, however, was executed during the conformational rearrangement of the envelope protein that occurs on the cell surface following attachment to the receptor and facilitates the exposure of HRs but not later than the transport into the endosome, where the avian leucosis sarcoma virus genome enters the cytoplasm by its envelope and endosomal membrane fusion in a low-pH environment (19, 22, 23). These observations together with those of the present study and others (1, 18, 24, 45) suggest that the HRPs have very low or little inhibitory effect in the endosome. If the above assumption is correct and the HRPs were designed to be efficiently transferred into the endosome and to be stable in the environment, they may be new antiviral candidates against those viruses that take the endosomal entry pathway, such as influenza virus, Ebola virus, and SCoV. Thus, detailed molecular studies on SCoV and the sHRP will provide a good model for the development and evaluation of such endosome-philic antiviral peptide inhibitors.

Recent studies have reported that the low inhibitory effect of the SCoV sHRP compared to that of the MHV HRP could be attributed to the weaker interaction of the SCoV S HR1-HR2 complex versus that of MHV S (1, 2). However, SCoV infection was efficiently blocked by sHRP under certain conditions, as revealed in this study; the concentration of sHRPs needed to inhibit SCoV infection is even lower than that required for MHV inhibition (1, 2). The apparent difference between MHV and SCoV infection is the pathway used to enter cells; the former enters directly from the cell surface, whereas the latter takes an endosomal pathway. Both MHV and SCoV infections were efficiently blocked when these viruses utilized the cell surface pathway for entry. These observations suggest that the lower HRP inhibitory effect on SCoV could be due to different entry pathways between SCoV and MHV rather than the weaker interaction of the HRP and SCoV S. To further explore this possibility, studies are ongoing to determine the effect of MHV sHRPs on infection by MHV-2, which, like SCoV, utilizes an endosomal infection pathway (29).

We thank Miyuki Kawase for her excellent technical assistance and Shutoku Matsuyama for his valuable discussions.

This work was financially supported by grants from the Ministry of Education, Culture, Sports, Science and Technology.

REFERENCES

1. **Bosch, B. J., B. E. Martina, R. Van Der Zee, J. Lepault, B. J. Haijema, C. Versluis, A. J. Heck, R. De Groot, A. D. Osterhaus, and P. J. Rottier.** 2004. Severe acute respiratory syndrome coronavirus (SARS-CoV) infection inhibition using spike protein heptad repeat-derived peptides. Proc. Natl. Acad. Sci. USA **101**:8455–8460.
2. **Bosch, B. J., R. van der Zee, C. A. de Haan, and P. J. Rottier.** 2003. The coronavirus spike protein is a class I virus fusion protein: structural and functional characterization of the fusion core complex. J. Virol. **77**:8801–8811.
3. **Chan, W. E., C. K. Chuang, S. H. Yeh, M. S. Chang, and S. S. Chen.** 2006. Functional characterization of heptad repeat 1 and 2 mutants of the spike protein of severe acute respiratory syndrome coronavirus. J. Virol. **80**:3225–3237.
4. **Drosten, C., S. Gunther, W. Preiser, S. van der Werf, H. R. Brodt, S. Becker, H. Rabenau, M. Panning, L. Kolesnikova, R. A. Fouchier, A. Berger, A. M. Burguiere, J. Cinatl, M. Eickmann, N. Escriou, K. Grywna, S. Kramme, J. C. Manuguerra, S. Muller, V. Rickerts, M. Sturmer, S. Vieth, H. D. Klenk, A. D. Osterhaus, H. Schmitz, and H. W. Doerr.** 2003. Identification of a novel coronavirus in patients with severe acute respiratory syndrome. N. Engl. J. Med. **348**:1967–1976.
5. **Earp, L. J., S. E. Delos, R. C. Netter, P. Bates, and J. M. White.** 2003. The avian retrovirus avian sarcoma/leukosis virus subtype A reaches the lipid mixing stage of fusion at neutral pH. J. Virol. **67**:3058–3066.
6. **Follis, K. E., J. York, and J. H. Nunberg.** 2005. Serine-scanning mutagenesis studies of the C-terminal heptad repeats in the SARS coronavirus S glycoprotein highlight the important role of the short helical region. Virology **341**:122–129.
7. **Fouchier, R. A., T. Kuiken, M. Schutten, G. van Amerongen, G. J. van Doornum, B. G. van den Hoogen, M. Peiris, W. Lim, K. Stohr, and A. D. Osterhaus.** 2003. Aetiology: Koch's postulates fulfilled for SARS virus. Nature **423**:240.
8. **Huang, I. C., B. J. Bosch, F. Li, W. Li, K. H. Lee, S. Ghiran, N. Vasilieva, T. S. Dermody, S. C. Harrison, P. R. Dormitzer, M. Farzan, P. J. Rottier, and H. Choe.** 2006. SARS coronavirus, but not human coronavirus NL63, utilizes cathepsin L to infect ACE2-expressing cells. J. Biol. Chem. **281**:3198–3203.
9. **Inoue, Y., N. Tanaka, Y. Tanaka, S. Inoue, K. Morita, M. Zhuang, T. Hattori, and K. Sugamura.** 2007. Clathrin-dependent entry of severe acute respira-

tory syndrome coronavirus into target cells expressing ACE2 with the cytoplasmic tail deleted. J. Virol. **81**:8722–8729.
10. **Jahn, R., T. Lang, and T. C. Sudhof.** 2003. Membrane fusion. Cell **112**:519–533.
11. **Jiang, S., K. Lin, N. Strick, and A. R. Neurath.** 1993. HIV-1 inhibition by a peptide. Nature **365**:113.
12. **Joshi, S. B., R. E. Dutch, and R. A. Lamb.** 1998. A core trimer of the paramyxovirus fusion protein: parallels to influenza virus hemagglutinin and HIV-1 gp41. Virology **248**:20–34.
13. **Kawabata, K., T. Hagio, and S. Matsuoka.** 2002. The role of neutrophil elastase in acute lung injury. Eur. J. Pharmacol. **451**:1–10.
14. **Kilby, J. M., S. Hopkins, T. M. Venetta, B. DiMassimo, G. A. Cloud, J. Y. Lee, L. Alldredge, E. Hunter, D. Lambert, D. Bolognesi, T. Matthews, M. R. Johnson, M. A. Nowak, G. M. Shaw, and M. S. Saag.** 1998. Potent suppression of HIV-1 replication in humans by T-20, a peptide inhibitor of gp41-mediated virus entry. Nat. Med. **4**:1302–1307.
15. **Ksiazek, T. G., D. Erdman, C. S. Goldsmith, S. R. Zaki, T. Peret, S. Emery, S. Tong, C. Urbani, J. A. Comer, W. Lim, P. E. Rollin, S. F. Dowell, A. E. Ling, C. D. Humphrey, W. J. Shieh, J. Guarner, C. D. Paddock, P. Rota, B. Fields, J. DeRisi, J. Y. Yang, N. Cox, J. M. Hughes, J. W. LeDuc, W. J. Bellini, and L. J. Anderson.** 2003. A novel coronavirus associated with severe acute respiratory syndrome. N. Engl. J. Med. **348**:1953–1966.
16. **Lambert, D. M., S. Barney, A. L. Lambert, K. Guthrie, R. Medinas, D. E. Davis, T. Bucy, J. Erickson, G. Merutka, and S. R. Petteway, Jr.** 1996. Peptides from conserved regions of paramyxovirus fusion (F) proteins are potent inhibitors of viral fusion. Proc. Natl. Acad. Sci. USA **93**:2186–2191.
17. **Li, F., M. Berardi, W. Li, M. Farzan, P. R. Dormitzer, and S. C. Harrison.** 2006. Conformational states of the severe acute respiratory syndrome coronavirus spike protein ectodomain. J. Virol. **80**:6794–6800.
18. **Liu, S., G. Xiao, Y. Chen, Y. He, J. Niu, C. R. Escalante, H. Xiong, J. Farmar, A. K. Debnath, P. Tien, and S. Jiang.** 2004. Interaction between heptad repeat 1 and 2 regions in spike protein of SARS-associated coronavirus: implications for virus fusogenic mechanism and identification of fusion inhibitors. Lancet **363**:938–947.
19. **Matsuyama, S., S. E. Delos, and J. M. White.** 2004. Sequential roles of receptor binding and low pH in forming prehairpin and hairpin conformations of a retroviral envelope glycoprotein. J. Virol. **78**:8201–8209.
20. **Matsuyama, S., M. Ujike, S. Morikawa, M. Tashiro, and F. Taguchi.** 2005. Protease-mediated enhancement of severe acute respiratory syndrome coronavirus infection. Proc. Natl. Acad. Sci. USA **102**:12543–12547.
21. **Medinas, R. J., D. M. Lambert, and W. A. Tompkins.** 2002. C-Terminal gp40 peptide analogs inhibit feline immunodeficiency virus: cell fusion and virus spread. J. Virol. **76**:9079–9086.
22. **Melikyan, G. B., R. J. Barnard, R. M. Markosyan, J. A. Young, and F. S. Cohen.** 2004. Low pH is required for avian sarcoma and leukosis virus Env-induced hemifusion and fusion pore formation but not for pore growth. J. Virol. **78**:3753–3762.
23. **Netter, R. C., S. M. Amberg, J. W. Balliet, M. J. Biscone, A. Vermeulen, L. J. Earp, J. M. White, and P. Bates.** 2004. Heptad repeat 2-based peptides inhibit avian sarcoma and leukosis virus subgroup a infection and identify a fusion intermediate. J. Virol. **78**:13430–13439.
24. **Ni, L., J. Zhu, J. Zhang, M. Yan, G. F. Gao, and P. Tien.** 2005. Design of recombinant protein-based SARS-CoV entry inhibitors targeting the heptad-repeat regions of the spike protein S2 domain. Biochem. Biophys. Res. Commun. **330**:39–45.
25. **Nicholls, J. M., L. L. Poon, K. C. Lee, W. F. Ng, S. T. Lai, C. Y. Leung, C. M. Chu, P. K. Hui, K. L. Mak, W. Lim, K. W. Yan, K. H. Chan, N. C. Tsang, Y. Guan, K. Y. Yuen, and J. S. Peiris.** 2003. Lung pathology of fatal severe acute respiratory syndrome. Lancet **361**:1773–1778.
26. **Nie, Y., P. Wang, X. Shi, G. Wang, J. Chen, A. Zheng, W. Wang, Z. Wang, X. Qu, M. Luo, L. Tan, X. Song, X. Yin, J. Chen, M. Ding, and H. Deng.** 2004. Highly infectious SARS-CoV pseudotyped virus reveals the cell tropism and its correlation with receptor expression. Biochem. Biophys. Res. Commun. **321**:994–1000.
27. **Otaka, A., M. Nakamura, D. Nameki, E. Kodama, S. Uchiyama, S. Nakamura, H. Nakano, H. Tamamura, Y. Kobayashi, M. Matsuoka, and N. Fujii.** 2002. Remodeling of gp41-C34 peptide leads to highly effective inhibitors of the fusion of HIV-1 with target cells. Angew. Chem. Int. Ed. Engl. **41**:2937–2940.
28. **Petit, C. M., J. M. Melancon, V. N. Chouljenko, R. Colgrove, M. Farzan, D. M. Knipe, and K. G. Kousoulas.** 2005. Genetic analysis of the SARS-coronavirus spike glycoprotein functional domains involved in cell-surface expression and cell-to-cell fusion. Virology **341**:215–230.
29. **Qiu, Z., S. T. Hingley, G. Simmons, C. Yu, J. Das Sarma, P. Bates, and S. R. Weiss.** 2006. Endosomal proteolysis by cathepsins is necessary for murine coronavirus mouse hepatitis virus type 2 spike-mediated entry. J. Virol. **80**:5768–5776.
30. **Rapaport, D., M. Ovadia, and Y. Shai.** 1995. A synthetic peptide corresponding to a conserved heptad repeat domain is a potent inhibitor of Sendai virus-cell fusion: an emerging similarity with functional domains of other viruses. EMBO J. **14**:5524–5531.
31. **Rota, P. A., M. S. Oberste, S. S. Monroe, W. A. Nix, R. Campagnoli, J. P. Icenogle, S. Penaranda, B. Bankamp, K. Maher, M. H. Chen, S. Tong, A. Tamin, L. Lowe, M. Frace, J. L. DeRisi, Q. Chen, D. Wang, D. D. Erdman, T. C. Peret, C. Burns, T. G. Ksiazek, P. E. Rollin, A. Sanchez, S. Liffick, B. Holloway, J. Limor, K. McCaustland, M. Olsen-Rasmussen, R. Fouchier, S. Gunther, A. D. Osterhaus, C. Drosten, M. A. Pallansch, L. J. Anderson, and W. J. Bellini.** 2003. Characterization of a novel coronavirus associated with severe acute respiratory syndrome. Science **300**:1394–1399.
32. **Sagara, Y., Y. Inoue, H. Shiraki, A. Jinno, H. Hoshino, and Y. Maeda.** 1996. Identification and mapping of functional domains on human T-cell lymphotropic virus type I envelope proteins by using synthetic peptides. J. Virol. **70**:1564–1569.
33. **Simmons, G., D. N. Gosalia, A. J. Rennekamp, J. D. Reeves, S. L. Diamond, and P. Bates.** 2005. Inhibitors of cathepsin L prevent severe acute respiratory syndrome coronavirus entry. Proc. Natl. Acad. Sci. USA **102**:11876–11881.
34. **Simmons, G., J. D. Reeves, A. J. Rennekamp, S. M. Amberg, A. J. Piefer, and P. Bates.** 2004. Characterization of severe acute respiratory syndrome-associated coronavirus (SARS-CoV) spike glycoprotein-mediated viral entry. Proc. Natl. Acad. Sci. USA **101**:4240–4245.
35. **Supekar, V. M., C. Bruckmann, P. Ingallinella, E. Bianchi, A. Pessi, and A. Carfi.** 2004. Structure of a proteolytically resistant core from the severe acute respiratory syndrome coronavirus S2 fusion protein. Proc. Natl. Acad. Sci. USA **101**:17958–17963.
36. **Wang, E., X. Sun, Y. Qian, L. Zhao, P. Tien, and G. F. Gao.** 2003. Both heptad repeats of human respiratory syncytial virus fusion protein are potent inhibitors of viral fusion. Biochem. Biophys. Res. Commun. **302**:469–475.
37. **Watanabe, S., A. Takada, T. Watanabe, H. Ito, H. Kida, and Y. Kawaoka.** 2000. Functional importance of the coiled-coil of the Ebola virus glycoprotein. J. Virol. **74**:10194–10201.
38. **Wild, C., T. Oas, C. McDanal, D. Bolognesi, and T. Matthews.** 1992. A synthetic peptide inhibitor of human immunodeficiency virus replication: correlation between solution structure and viral inhibition. Proc. Natl. Acad. Sci. USA **89**:10537–10541.
39. **Wild, C. T., D. C. Shugars, T. K. Greenwell, C. B. McDanal, and T. J. Matthews.** 1994. Peptides corresponding to a predictive alpha-helical domain of human immunodeficiency virus type 1 gp41 are potent inhibitors of virus infection. Proc. Natl. Acad. Sci. USA **91**:9770–9774.
40. **Xu, Y., Z. Lou, Y. Liu, H. Pang, P. Tien, G. F. Gao, and Z. Rao.** 2004. Crystal structure of severe acute respiratory syndrome coronavirus spike protein fusion core. J. Biol. Chem. **279**:49414–49419.
41. **Yang, Z. Y., Y. Huang, L. Ganesh, K. Leung, W. P. Kong, O. Schwartz, K. Subbarao, and G. J. Nabel.** 2004. pH-dependent entry of severe acute respiratory syndrome coronavirus is mediated by the spike glycoprotein and enhanced by dendritic cell transfer through DC-SIGN. J. Virol. **78**:5642–5650.
42. **Yao, Q., and R. W. Compans.** 1996. Peptides corresponding to the heptad repeat sequence of human parainfluenza virus fusion protein are potent inhibitors of virus infection. Virology **223**:103–112.
43. **Young, J. K., D. Li, M. C. Abramowitz, and T. G. Morrison.** 1999. Interaction of peptides with sequences from the Newcastle disease virus fusion protein heptad repeat regions. J. Virol. **73**:5945–5956.
44. **Yu, M., E. Wang, Y. Liu, D. Cao, N. Jin, C. W. Zhang, M. Bartlam, Z. Rao, P. Tien, and G. F. Gao.** 2002. Six-helix bundle assembly and characterization of heptad repeat regions from the F protein of Newcastle disease virus. J. Gen. Virol. **83**:623–629.
45. **Yuan, K., L. Yi, J. Chen, X. Qu, T. Qing, X. Rao, P. Jiang, J. Hu, Z. Xiong, Y. Nie, X. Shi, W. Wang, C. Ling, X. Yin, K. Fan, L. Lai, M. Ding, and H. Deng.** 2004. Suppression of SARS-CoV entry by peptides corresponding to heptad regions on spike glycoprotein. Biochem. Biophys. Res. Commun. **319**:746–752.

CHEMBIOCHEM

DOI: 10.1002/cbic.200700761

Synthesis and Application of Fluorescein- and Biotin-Labeled Molecular Probes for the Chemokine Receptor CXCR4

Shinya Oishi,*[a] Ryo Masuda,[a] Barry Evans,[b] Satoshi Ueda,[a] Yukiko Goto,[a] Hiroaki Ohno,[a] Akira Hirasawa,[a] Gozoh Tsujimoto,[a] Zixuan Wang,[b] Stephen C. Peiper,[b] Takeshi Naito,[c] Eiichi Kodama,[c] Masao Matsuoka,[c] and Nobutaka Fujii*[a]

The design, synthesis, and bioevaluation of fluorescence- and biotin-labeled CXCR4 antagonists are described. The modification of D-Lys8 at an ε-amino group in the peptide antagonist Ac-TZ14011 derived from polyphemusin II had no significant influence on the potent binding of the peptide to the CXCR4 receptor. The application of the labeled peptides in flow cytometry and confocal microscopy studies demonstrated the selectivity of their binding to the CXCR4 receptor, but not to CXCR7, which was recently reported to be another receptor for stromal cell-derived factor 1 (SDF-1)/CXCL12.

Introduction

The CXC chemokine receptor 4 (CXCR4) is a G-protein-coupled cell-surface receptor that was identified previously as a coreceptor for infection by the T-cell-line-tropic (X4) human immunodeficiency virus type 1 (HIV-1).[1,2] Stromal cell-derived factor 1 (SDF-1)/CXCL12 is a homeostatic chemokine that regulates a number of physiological and pathologic processes through its interaction with and activation of CXCR4. SDF-1 secreted in bone-marrow stromal cells supports the retention of hematopoietic stem cells (HSCs), progenitor cells, and B-cell precursors in the hematopoietic microenvironment.[3] SDF-1 expression is implicated in the survival, growth, and development of CXCR4-expressing cells, including normal and malignant B lymphocytes, hematopoietic progenitors, and carcinoma cells.[3,4] It has also been demonstrated that concentration gradients of SDF-1 promote the homing of HSCs to bone marrow, the recruitment of progenitor cells to sites of ischemic tissue damage, and the metastasis of CXCR4-expressing neoplastic cells to target organs.[4,5]

Recently, CXCR7 (RDC1, CCX-CKR2) was reported to be another receptor for SDF-1.[6,7] CXCR7 promotes cell survival, growth, and adhesion in vitro and in vivo.[7,8] Furthermore, the expression pattern of CXCR7 is complementary to that of CXCR4 in the migrating primordium.[9,10] Therefore, the SDF-1–CXCR7 axis, like SDF-1–CXCR4, is relevant to the control processes of cell growth, migration, and recruitment. To investigate the distribution and localization of two binding partners of SDF-1, CXCR4 and CXCR7, both in vitro and in vivo, it would be useful to have access to selective and specific fluorescence- and otherwise-labeled ligands for these receptors.

To date, several CXCR4-receptor probes have been prepared and applied both in vitro[11–14] and in vivo.[15] Fluorescein-labeled SDF-1 was utilized to detect the CXCR4-dependent internalization of SDF-1 by stromal bone-marrow cells.[11] This labeled agonist was useful for evaluating the mechanism of receptor activation. We developed a potential radiopharmaceutical agent based on the polyphemusin II derived CXCR4 antagonist T140 (Scheme 1). Thus, [^{111}In]-diethylenetriaminepenta-

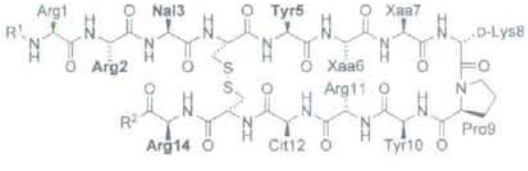

	R^1	R^2	Xaa6	Xaa7
T140	H	OH	Arg	Lys
Ac-TZ14011 (**1**)	Ac	NH_2	Cit	Arg

Scheme 1. Structure of the selective CXCR4 antagonists T140, which was used to design probe Ac-TZ14011 (**1**). Bold type indicates the pharmacophore residues.

[a] Dr. S. Oishi, R. Masuda, Dr. S. Ueda, Y. Goto, Dr. H. Ohno, Dr. A. Hirasawa, Prof. Dr. G. Tsujimoto, Prof. Dr. N. Fujii
Graduate School of Pharmaceutical Sciences, Kyoto University
Sakyo-ku, Kyoto 606-8501 (Japan)
Fax: (+81) 75-753-4570
E-mail: soishi@pharm.kyoto-u.ac.jp
nfujii@pharm.kyoto-u.ac.jp

[b] B. Evans, Dr. Z. Wang, Prof. Dr. S. C. Peiper
Department of Pathology, Medical College of Georgia
Georgia 30912 (USA)

[c] T. Naito, Dr. E. Kodama, Prof. Dr. M. Matsuoka
Institute for Virus Research, Kyoto University
Sakyo-ku, Kyoto 606-8507 (Japan)

Supporting information for this article is available on the WWW under http://www.chembiochem.org or from the author.

acetic acid (DTPA) labeled Ac-TZ14011 was designed for the in vivo imaging of CXCR4-expressing tumors.[15] Rhodamine-conjugated azamacrocycle antagonists were also developed; however, the small molecules were taken up into the cells by a potential active-transport process.[13]

On the basis of our previous research on peptide-based CXCR4 antagonists,[16] we conducted an extensive structure–activity-relationship analysis of labeled ligands with CXCR4 receptors expressed on the cell surface. Herein, we report the design of the labeled antagonists and their application in in vitro experiments, including flow cytometry. The selectivity of the ligand for CXCR4 versus CXCR7 was also investigated by confocal microscopy.

Results and Discussion

Peptide design and synthesis

Previous alanine-scanning experiments identified four indispensable pharmacophore residues of T140, which are located peripheral to the disulfide bridge.[17] On the other hand, modification of the N and C termini or β-turn region with several types of functional groups or peptidomimetics did not lead to a decrease in activity.[16] For example, arylacyl functional groups, such as fluorobenzoyl, at the N terminus of T140 analogues enhanced anti-HIV activity.[18] On the basis of these precedent structure–activity-relationship studies on T140 derivatives, we designed two types of potential labeled CXCR4 ligands (Tables 1 and 2). The functional groups for labeling were attached with an appropriate spacer by acylation to the α-amino group of the N-terminal Arg1 residue or on the ε-amino group of D-Lys8. To identify appropriate fluorophores that did not affect peptide binding affinity to CXCR4, carboxyfluorescein and Alexa Fluor 488, which have a similar fluorescence spectrum, were used for fluorescence labeling. The different functional groups on the fluorescent section of peptides could have an effect on the affinities of the peptides for CXCR4. The Alexa Fluor 488 dye, which contains an amino group, an imino group, and two sulfonate groups on a xanthene structure, exhibited greater photostability and pH insensitivity.

Peptide resins were constructed manually by standard Fmoc-based solid-phase peptide synthesis (SPPS) by using *N,N'*-diisopropylcarbodiimide (DIC)/1-hydroxybenzotriazole (HOBt). Fluorescein or acetyl modification at the N-terminal α-amino group of peptides **1**–**4** was carried out on the resin by using carboxyfluorescein/DIC/HOBt or Ac_2O/pyridine, respectively. For the preparation of peptides **6**–**8** and **10** with either a fluorescein label or a 6-aminocaproic acid (Acp) linker combined with a fluorescein, biotin, or Alexa Fluor 488 label on the ε-amino group of D-Lys8, a 4-methyltrityl (Mtt) group was used for side-chain protection (Scheme 2). After the removal of the Mtt group on peptide **11** with 1,1,1,3,3,3-hexafluoropropan-2-ol (HFIP), an Acp linker and/or labeling groups were attached to the peptide resin **12** by a standard protocol to afford the labeled protected peptide resins **13**–**16**. Treatment of the protected peptide resins with TFA/1,2-ethanedithiol (EDT)/H_2O (95:2.5:2.5) followed by air oxidation in aqueous solution yielded the expected peptides **1**–**4**, **6**–**8**, and **17**.

Labeling with Alexa Fluor 488 was performed with the activated succinimidyl ester, which is commercially available. The

Table 1. Sequences and biological activity of labeled T140 analogues.

R-Arg-Arg-Nal-Cys-Tyr-Cit-Arg-D-**Xaa**-Pro-Tyr-Arg-Cit-Cys-Arg-NH_2

Peptide	R	D-Xaa	IC_{50} [nM][a]
1	Ac	D-Lys	5.2 ± 0.1
2	Ac	D-Glu	6.7 ± 2.6
3	fluorescein	D-Lys	24 ± 0.3
4	fluorescein	D-Glu	199 ± 26
5	Alexa Fluor 488	D-Glu	5700 ± 769

[a] IC_{50} values for the peptides are based on the inhibition of [^{125}I]SDF-1 binding to CHO cells that were transfected with CXCR4.

Table 2. Sequences and biological activity of Ac-TZ14011 analogues.

Ac-Arg-Arg-Nal-Cys-Tyr-Cit-Arg-D-**Lys**-Pro-Tyr-Arg-Cit-Cys-Arg-NH_2 (R on Lys)

Peptide	R	IC_{50} [nM][a]
1	H (amine)	5.2 ± 0.1
6	fluorescein	16 ± 0.8
7	fluorescein-Acp-	26 ± 2.4
8	biotin-Acp-	11 ± 0.1
9	Alexa Fluor 488	8.1 ± 3.5
10	Alexa Fluor 488-Acp-	267 ± 19

[a] IC_{50} values for the peptides are based on the inhibition of [^{125}I]SDF-1 binding to CHO cells that were transfected with CXCR4.

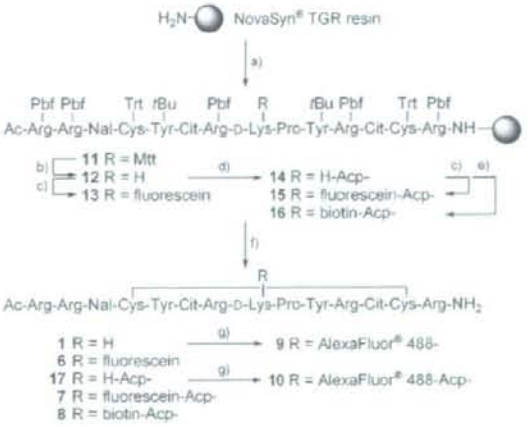

Scheme 2. Synthesis of D-Lys8-labeled CXCR4 antagonists: a) Fmoc-based peptide synthesis; b) CH_2Cl_2/HFIP/TFE/TES (65:20:10:5); c) carboxyfluorescein, DIC, HOBt; d) Fmoc-Acp-OH, DIC, HOBt, then 20% piperidine/DMF; e) biotin, DIC, HOBt; f) TFA/EDT/H_2O (95:2.5:2.5), then NH_4OH; g) Alexa Fluor 488–OSu, iPr_2NEt. DMF: *N,N*-dimethylformamide; Fmoc: 9-fluorenylmethoxycarbonyl; Pbf: 2,2,4,6,7-pentamethyldihydrobenzofuran-5-sulfonyl; TFE: 2,2,2-trifluoroethanol; TES: triethylsilane; Trt: triphenylmethyl (trityl).

precursor peptides (e.g., **1**, **17**) were modified in DMF to provide the expected peptides **5**, **9**, and **10** with a single Alexa Fluor 488 dye moiety.[19]

Biological evaluation of fluorescein- and biotin-labeled peptides

The CXCR4-antagonistic activity of peptides **1**–**10** was evaluated with respect to the inhibition of [^{125}I]SDF-1 binding to CXCR4 Chinese hamster ovary (CHO) cell transfectants. The replacement of D-Lys8 in the parent peptide **1** with D-glutamic acid had no significant effect on the bioactivity of the peptide (IC_{50}(**1**) = 5.2 nM; IC_{50}(**2**) = 6.7 nM; Table 1); this is consistent with the results of previous Glu-scanning experiments of a related peptide.[20] This result suggested that the modification of the β turn $i+1$ position of the peptides with a functional group for labeling would be possible. Fluorescein modification of the N terminus of peptides **1** and **2** led to a slight and significant decrease in inhibitory activity (IC_{50}(**3**) = 24 nM; IC_{50}(**4**) = 199 nM), respectively. Although the substituted benzoyl and pyridinecarbonyl groups at the N terminus of the peptide improved its bioactivity,[18] an additional xanthene or carboxyl group might be unfavorable to ligand binding with CXCR4. The Alexa Fluor 488 labeled peptide **5** showed a significant decrease in inhibitory activity (IC_{50}(**5**) = 5.7 μM); this indicates that the N terminus is inappropriate for fluorescence labeling.

Modification of the ε-amino group of D-Lys8 in the parent peptide **1** was another promising approach to the creation of labeled CXCR4 antagonists (Table 2). The fluorescein-modified peptides **6** and **7** exhibited slightly decreased bioactivity but retained significant binding affinity for CXCR4 (IC_{50}(**6**) = 16 nM; IC_{50}(**7**) = 26 nM). The biotin-labeled peptide **8** containing an Acp spacer, which would be helpful for the simultaneous binding of **8** with CXCR4 and avidins, was also a potent inhibitor (IC_{50}(**8**) = 11 nM). Thus, the presence of a functional group at this position for labeling, with or without an Acp spacer, did not appear to influence the bioactivity of the peptide. We concluded that the D-Lys8 residue in the β-turn region might be unimportant for direct molecular recognition by CXCR4; consequently, this position was considered to be more appropriate for labeling. The Alexa Fluor 488 labeled peptide **9** without an Acp linker showed nearly equipotent inhibitory activity to that of the parent peptide **1** (IC_{50}(**9**) = 8.1 nM). In contrast, significantly lower bioactivity was observed for peptide **10**, which contains an Acp linker (IC_{50}(**10**) = 267 nM). This result implies that the modified xanthene structure of Alexa Fluor 488 might cause some unfavorable interactions with the receptor, contrary to our expectations. The two potent labeled peptides **6** and **9** were used for further experiments.

Application of fluorescence-labeled peptides to flow cytometry and confocal microscopy studies

The applicability of the fluorescence-labeled CXCR4 antagonists **6** and **9** to in vitro experiments was investigated (Figure 1A and B). CHO cells that expressed high levels of the CXCR4 receptor and CXCR4-negative control cells were incubated with peptide **6** or **9** (200 nM), and the resulting mixtures were analyzed by flow cytometry. The CXCR4-expressing cells bound the fluorescent ligand, but the cells that did not express CXCR4 were not stained. The binding of peptides **6** and **9** was inhibited by competition with the unlabeled specific CXCR4 antagonist T140 (200 nM). This result supports the specificity of the fluorescent ligands for CXCR4. With the fluorescent probe **6**, lymphocytes derived from mouse spleen were identified by light scatter gating and analyzed for binding of the fluorescent antagonists (Figure 1C). Peptide **6** bound to CXCR4-expressing lymphocytes, and the staining was inhibited competitively by the addition of unlabeled T140 (200 nM). Peptide **6** was also utilized for the detection of chemotactic cells in a transmigration assay with CXCL12 (Figure 1D). Whereas a low percentage of the cells in the top well of a chemotaxis chamber were positive, the cells which passed through 3-μm pores in response to the CXCL12 chemotactic gradient were all stained positively with peptide **6**.

The probing ability of **6** and **9** for CXCR4 was also verified by confocal microscopy studies on CXCR4-expressing HEK293 cells (Figure 2). The cell surface of CXCR4-positive cells was stained with peptides **6** and **9** in a dose-dependent manner (Figure 2A; see also the Supporting Information). This result is in contrast to a previous report that a rhodamine-labeled azamacrocycle localizes in the cytoplasm by nonspecific uptake.[13] Staining was not observed with CXCR4-negative control cells; this suggests that receptor recognition of these fluorescent peptides is specific to CXCR4 (Figure 2C). Furthermore, CXCR7-expressing HEK293 cells were not stained by the fluorescent peptides **6** and **9** (Figure 2B); this indicates that these T140 derivatives are selective inhibitors of the CXCR4 receptor.

Conclusions

In the current study the effects of labeling a peptide at different positions with various functionalities with a view to retaining indispensable interactions with the CXCR4 receptor was investigated. Fluorescein, biotin, and Alexa Fluor 488 moieties on the D-Lys8 ε-amino group of the parent peptide were appropriate labels. The resulting labeled peptides exhibited specific and high affinity for the CXCR4 receptor, but not for the CXCR7 receptor. The labeled peptides could be useful as selective molecular probes for the CXCR4 receptor in future in vitro and/or in vivo experiments.

Experimental Section

General procedure for peptide synthesis: Protected peptide resins were constructed manually by standard Fmoc-based SPPS on NovaSyn TGR resin (192 mg, 0.05 mmol) by using DIC (39 μL, 0.25 mmol) in combination with HOBt (38 mg, 0.25 mmol). The side chains Tyr, Glu, Lys, Cys, and Arg were protected with *t*Bu, *t*Bu ester, Boc, Trt, and Pbf groups, respectively. For the preparation of peptides **6**–**8** and **10**, the Mtt group was used to protect the D-Lys8 side chain. The N-terminal α-amino group was acetylated by treatment of the resin with Ac_2O (24 μL, 0.25 mmol) and pyridine (40 μL, 0.10 mmol). Biotin (61 mg, 0.25 mmol) or carboxyfluorescein (94 mg, 0.25 mmol) was coupled to the peptide by using DIC

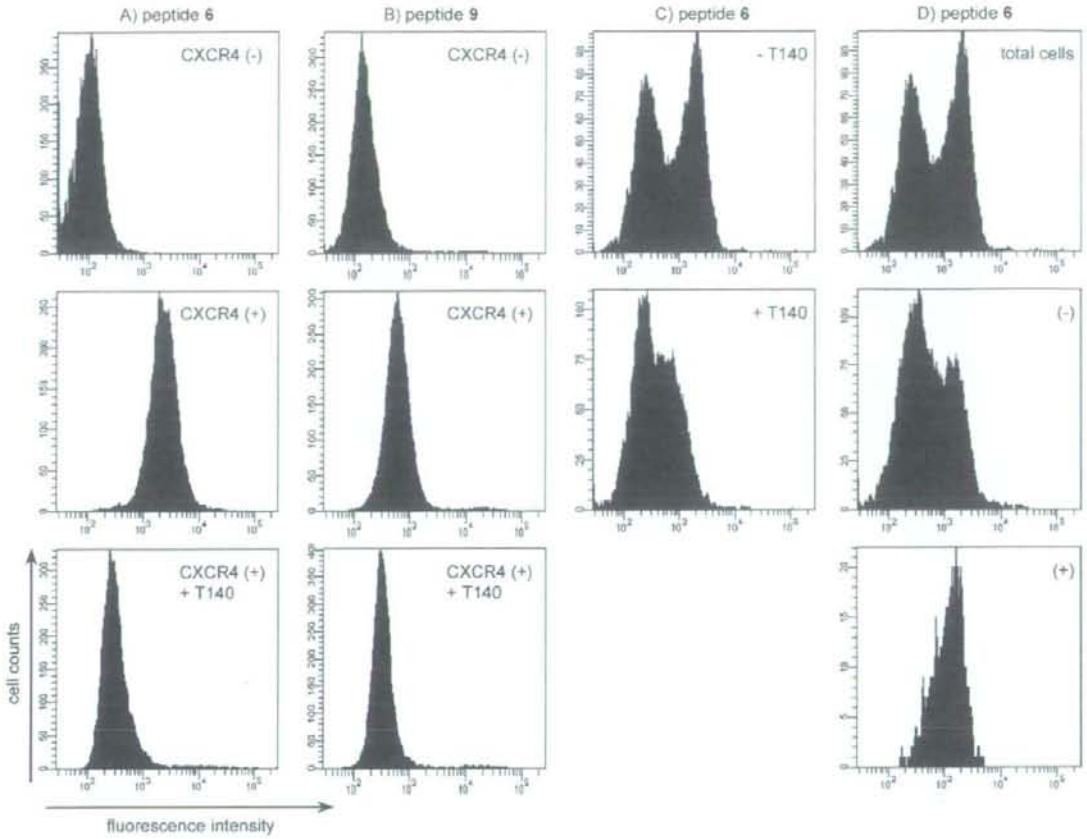

Figure 1. Application of fluorescent CXCR4 antagonists **6** and **9** to flow cytometry. CHO cells were incubated with labeled peptides (200 nM) A) **6**, and B) **9**. The top and middle panels show the results with cells that did not (–) and did express CXCR4 (+), respectively. Competitive binding was assessed with T140 (200 nM; lower panels). C) FACS (fluorescence-activated cell sorting) data for mouse spleen cells treated with peptide **6** (200 nM) in the presence (+) and absence (–) of T140 (200 nM). D) Chemotaxis experiment with mouse spleen cells (top panel). Cells from the total population that did not display chemotaxis are shown in the middle panel (–), and cells that migrated in response to a gradient of SDF-1 are shown in the lower panel (+).

(39 μL, 0.25 mmol) and HOBt (38 mg, 0.25 mmol) in DMF (2 mL). The resulting protected peptide resin (0.05 mmol) was treated with TFA/H_2O/EDT (95:2.5:2.5, 4 mL) for 2 h at room temperature. After removal of the resin by filtration, ice-cold dry Et_2O (100 mL) was added to the residue. The resulting powder was collected by centrifugation and then washed with ice-cold dry Et_2O (3×50 mL). The crude reduced peptide was dissolved in H_2O (100 mL), and the pH value was adjusted to 8.0 with NH_4OH. After oxidation by exposure to air for 1 day, the crude product in the solution was purified by preparative HPLC to afford the desired peptide as a white powder.

Removal of the Mtt protecting group: The resin (0.05 mmol) was treated with CH_2Cl_2/HFIP/TFE/TES (6.5:2:1:0.5, 10 mL) for 2 h at room temperature. It was then washed with the same mixture twice, treated with 10% iPr_2NEt in DMF, and used for the next coupling.

Conjugation of Alexa Fluor 488 succinimidyl ester with peptides: Lyophilized peptide (4.66 μmol) and iPr_2NEt (3.77 μL, 27.2 μmol) were added to a solution of Alexa Fluor 488 succinimidyl ester (2.50 mg, 3.88 μmol) in DMF (250 μL), and the resulting mixture was stirred in the dark for 12 h at room temperature. The crude mixture was then diluted with MeOH (100 μL) and purified by HPLC. Fractions containing Alexa Fluor 488 conjugates were collected and lyophilized to give **5** (3.3 mg, 27%), **9** (5.1 mg, 51% from **1**), or **10** (5.88 mg, 46% from **17**) as a red powder.

Acknowledgements

This research was supported by a Grant-in-Aid for Scientific Research from the Ministry of Education, Culture, Sports, Science, and Technology of Japan, the 21st Century COE Program "Knowledge Information Infrastructure for Genome Science", and the Targeted Proteins Research Program. S.U. is grateful for a JSPS Research Fellowship for Young Scientists. We thank Maxwell Reback (Kyoto University) for reading the manuscript.

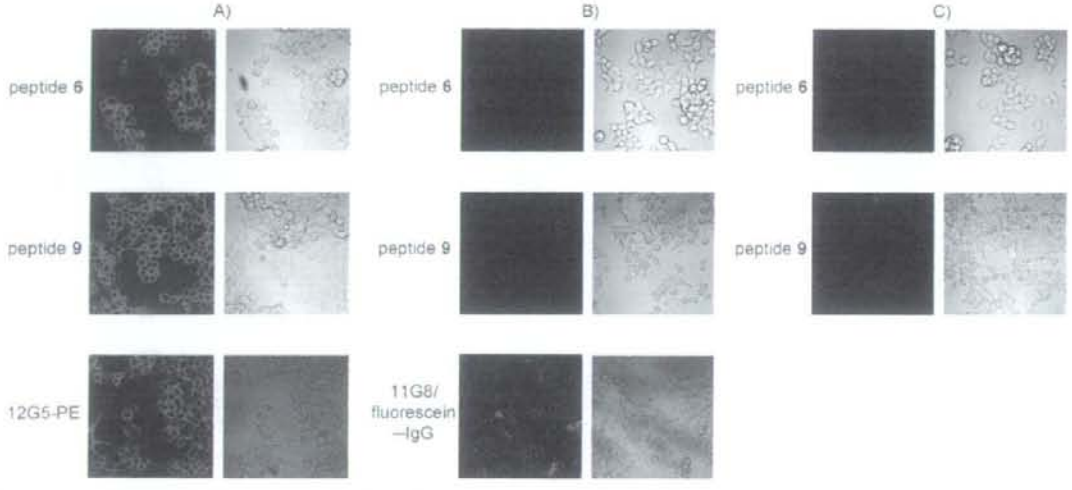

Figure 2. Confocal images of HEK293 cells stained with peptides **6** and **9** (100 nM): A) CXCR4-expressing cells, B) CXCR7-expressing cells, C) CXCR4-negative control cells. CXCR4- and CXCR7-receptor expression was verified by using the monoclonal antibodies 12G5 and 11G8.

Keywords: cell imaging · chemokine receptors · CXCR4 antagonists · fluorescent probes · peptides

[1] Y. Feng, C. C. Broder, P. E. Kennedy, E. A. Berger, *Science* **1996**, *272*, 872–877.
[2] E. Oberlin, A. Amara, F. Bachelerie, C. Bessia, J. L. Virelizier, F. Arenzana-Seisdedos, O. Schwartz, J. M. Heard, I. Clark-Lewis, D. F. Legler, M. Loetscher, M. Baggiolini, B. Moser, *Nature* **1996**, *382*, 833–835.
[3] T. Nagasawa, *Nat. Rev. Immunol.* **2006**, *6*, 107–116.
[4] J. A. Burger, T. J. Kipps, *Blood* **2006**, *107*, 1761–1767.
[5] T. Lapidot, A. Dar, O. Kollet, *Blood* **2005**, *106*, 1901–1910.
[6] K. Balabanian, B. Lagane, S. Infantino, K. Y. Chow, J. Harriague, B. Moepps, F. Arenzana-Seisdedos, M. Thelen, F. Bachelerie, *J. Biol. Chem.* **2005**, *280*, 35760–35766.
[7] J. M. Burns, B. C. Summers, Y. Wang, A. Melikian, R. Berahovich, Z. Miao, M. E. Penfold, M. J. Sunshine, D. R. Littman, C. J. Kuo, K. Wei, B. E. McMaster, K. Wright, M. C. Howard, T. J. Schall, *J. Exp. Med.* **2006**, *203*, 2201–2213.
[8] Z. Miao, K. E. Luker, B. C. Summers, R. Berahovich, M. S. Bhojani, A. Rehemtulla, C. G. Kleer, J. J. Essner, A. Nasevicius, G. D. Luker, M. C. Howard, T. J. Schall, *Proc. Natl. Acad. Sci. USA* **2007**, *104*, 15735–15740.
[9] C. Dambly-Chaudière, N. Cubedo, A. Ghysen, *BMC Dev. Biol.* **2007**, *7*, 23.
[10] G. Valentin, P. Haas, D. Gilmour, *Curr. Biol.* **2007**, *17*, 1026–1031.
[11] A. Dar, P. Goichberg, V. Shinder, A. Kalinkovich, O. Kollet, N. Netzer, R. Margalit, M. Zsak, A. Nagler, I. Hardan, I. Resnick, A. Rot, T. Lapidot, *Nat. Immunol.* **2005**, *6*, 1038–1046.
[12] O. Kollet, A. Dar, S. Shivtiel, A. Kalinkovich, K. Lapid, Y. Sztainberg, M. Tesio, R. M. Samstein, P. Goichberg, A. Spiegel, A. Elson, T. Lapidot, *Nat. Med.* **2006**, *12*, 657–664.
[13] A. Khan, J. D. Silversides, L. Madden, J. Greenman, S. J. Archibald, *Chem. Commun.* **2007**, 416–418.
[14] W. Zhan, Z. Liang, A. Zhu, S. Kurtkaya, H. Shim, J. P. Snyder, D. C. Liotta, *J. Med. Chem.* **2007**, *50*, 5655–5664.
[15] H. Hanaoka, T. Mukai, H. Tamamura, T. Mori, S. Ishino, K. Ogawa, Y. Iida, R. Doi, N. Fujii, H. Saji, *Nucl. Med. Biol.* **2006**, *33*, 489–494.
[16] H. Tsutsumi, T. Tanaka, N. Ohashi, H. Masuno, H. Tamamura, K. Hiramatsu, T. Araki, S. Ueda, S. Oishi, N. Fujii, *Biopolymers* **2007**, *88*, 279–289.
[17] H. Tamamura, A. Omagari, S. Oishi, T. Kanamoto, N. Yamamoto, S. C. Peiper, H. Nakashima, A. Otaka, N. Fujii, *Bioorg. Med. Chem. Lett.* **2000**, *10*, 2633–2637.
[18] H. Tamamura, K. Hiramatsu, M. Mizumoto, S. Ueda, S. Kusano, S. Terakubo, M. Akamatsu, N. Yamamoto, J. O. Trent, Z. Wang, S. C. Peiper, H. Nakashima, A. Otaka, N. Fujii, *Org. Biomol. Chem.* **2003**, *1*, 3663–3669.
[19] The fluorescent peptides **3–7**, **9**, and **10** contain the fluorescent labels in two regioisomeric forms derived from commercially available carboxyfluorescein and Alexa Fluor 488 succinimidyl ester.
[20] H. Tamamura, K. Hiramatsu, S. Kusano, S. Terakubo, N. Yamamoto, J. O. Trent, Z. Wang, S. C. Peiper, H. Nakashima, A. Otaka, N. Fujii, *Org. Biomol. Chem.* **2003**, *1*, 3656–3662.

Received: December 15, 2007
Published online on April 15, 2008

SOCS1 is an inducible host factor during HIV-1 infection and regulates the intracellular trafficking and stability of HIV-1 Gag

Akihide Ryo[a,b,c], Naomi Tsurutani[d], Kenji Ohba[b,e], Ryuichiro Kimura[e,f], Jun Komano[b], Mayuko Nishi[a], Hiromi Soeda[a], Shinichiro Hattori[b], Kilian Perrem[g], Mikio Yamamoto[h], Joe Chiba[f], Jun-ichi Mimaya[i], Kazuhisa Yoshimura[j], Shuzo Matsushita[j], Mitsuo Honda[b], Akihiko Yoshimura[k], Tatsuya Sawasaki[l], Ichiro Aoki[a], Yuko Morikawa[d], and Naoki Yamamoto[b,c]

[a]Department of Pathology, Yokohama City University School of Medicine, 3-9 Fuku-ura, Kanazawa-ku, Yokohama 236-0004, Japan; [b]AIDS Research Center, National Institute of Infectious Diseases, 1-23-1 Toyama, Shinjuku-ku, Tokyo 162-8640, Japan; [c]Kitasato Institute for Life Sciences, Kitasato University, Shirokane 5-9-1, Minato-ku, Tokyo 108-8641, Japan; [d]Department of Molecular Virology, Graduate School of Medicine, Tokyo Medical and Dental University, 1-5-45 Yushima, Bunkyo-ku, Tokyo 113-8519, Japan; [f]Molecular Oncology Laboratory, Department of Pathology, Royal College of Surgeons in Ireland, Smurfit Building, Beaumont Hospital, Dublin 9, Ireland; [h]Department of Biochemistry II, National Defense Medical College, 3-2 Namiki, Tokorozawa-shi, Saitama 359-8513, Japan; [g]Department of Biological Science and Technology, Science University of Tokyo, 2641 Yamazaki, Noda, Chiba 278-8510, Japan; [i]Division of Hematology and Oncology, Shizuoka Children's Hospital, 860 Urushiyama, Aoi-ku, Shizuoka 420-8660, Japan; [j]Division of Clinical Retrovirology and Infectious Diseases, Center for AIDS Research, Graduate School of Medical Sciences, Kumamoto University, Kumamoto 860-0811, Japan; [k]Division of Molecular and Cellular Immunology, Medical Institute of Bioregulation, Kyushu University, Fukuoka 812-8582, Japan; and [l]Cell Free Science and Research Center, Ehime University, Ehime 790-8577, Japan

Edited by Robert C. Gallo, University of Maryland, Baltimore, MD, and approved November 19, 2007 (received for review May 24, 2007)

Human immunodeficiency virus type 1 (HIV-1) utilizes the macromolecular machinery of the infected host cell to produce progeny virus. The discovery of cellular factors that participate in HIV-1 replication pathways has provided further insight into the molecular basis of virus–host cell interactions. Here, we report that the suppressor of cytokine signaling 1 (SOCS1) is an inducible host factor during HIV-1 infection and regulates the late stages of the HIV-1 replication pathway. SOCS1 can directly bind to the matrix and nucleocapsid regions of the HIV-1 p55 Gag polyprotein and enhance its stability and trafficking, resulting in the efficient production of HIV-1 particles via an IFN signaling-independent mechanism. The depletion of SOCS1 by siRNA reduces both the targeted trafficking and assembly of HIV-1 Gag, resulting in its accumulation as perinuclear solid aggregates that are eventually subjected to lysosomal degradation. These results together indicate that SOCS1 is a crucial host factor that regulates the intracellular dynamism of HIV-1 Gag and could therefore be a potential new therapeutic target for AIDS and its related disorders.

AIDS | pathogenesis | drug target | lysozyme

Human immunodeficiency virus type 1 (HIV-1) infection is a multistep and multifactorial process mediated by a complex series of virus–host cell interactions (1, 2). The molecular interactions between host cell factors and HIV-1 are vital to our understanding of not only the nature of the resulting viral replication, but also the subsequent cytopathogenesis that occurs in the infected cells (3). The characterization of the genes in the host cells that are up- or down-regulated upon HIV-1 infection could therefore provide a further elucidation of virus–host cell interactions and identify putative molecular targets for the HIV-1 replication pathway (4).

The HIV-1 p55 Gag protein consists of four domains that are cleaved by the viral protease concomitantly with virus release. This action generates the mature Gag protein comprising the matrix (MA/p17), capsid (CA/p24), nucleocapsid (NC/p7), and p6 domains, in addition to two small spacer peptides, SP1 and SP2 (5, 6). The N-terminal portion of MA, which is myristoylated, facilitates the targeting of Gag to the plasma membrane (PM), whereas CA and NC promote Gag multimerization. p6 plays a central role in the release of HIV-1 particles from PM by interacting with the vacuolar sorting protein Tsg101 and AIP1/ALIX (7–9). Several recent studies have implicated the presence of host factors in the control of the intracellular trafficking of Gag. AP-3δ is a recently characterized endosomal adaptor protein that binds directly to the MA region of Gag and enhances its targeting to the multivesicular body (MVB) during the early stages of particle assembly (10). The *trans*-Golgi network (TGN)-associated protein hPOSH plays another role in Gag transport by facilitating the egress of Gag cargo vesicles from the TGN, where it assembles with envelope protein (Env) before transport to PM (11). Although the involvement of these host proteins in the regulation of intracellular Gag trafficking has been proposed, the detailed molecular mechanisms underlying this process are still not yet well characterized.

In our current work, we demonstrate that the suppressor of cytokine signaling 1 (SOCS1) directly binds HIV-1 Gag and facilitates the intracellular trafficking and stability of this protein, resulting in the efficient production of HIV-1 particles. These results indicate that SOCS1 is a crucial host factor for efficient HIV-1 production and could be an intriguing molecular target for future treatment of AIDS and related diseases.

Results

SOCS1 Is Induced upon HIV-1 Infection and Facilitates HIV-1 Replication via Posttranscriptional Mechanisms. We and others have shown that HIV-1 infection can alter cellular gene expression patterns, resulting in the modification of viral replication and impaired homeostasis in the host cells (4, 12). Hence, to elucidate further the genes and cellular pathways that participate in HIV-1 replication processes, we performed serial analysis of gene expression (SAGE) using either a HIV-1 or mock-infected human T cell line, MOLT-4 (12). Further detailed analysis of relatively low-abundance SAGE tags identified *SOCS1* as a preferentially up-regulated gene after HIV-1 infection. This finding was validated by both semiquantitative RT-PCR and immunoblotting analysis with anti-SOCS1 anti-

Author contributions: A.R. and N.T. contributed equally to this work; A.R., A.Y., Y.M., and N.Y. designed research; A.R., N.T., K.O., R.K., M.N., H.S., S.H., T.S., I.A., and Y.M. performed research; J.K., S.H., M.Y., J.C., J.-i.M., K.Y., S.M., M.H., and A.Y. contributed new reagents/analytic tools; A.R., N.T., K.O., M.N., H.S., K.P., M.Y., K.Y., S.M., T.S., I.A., Y.M., and N.Y. analyzed data; and A.R., K.P., and N.Y. wrote the paper.

The authors declare no conflict of interest.

This article is a PNAS Direct Submission.

Freely available online through the PNAS open access option.

[1]To whom correspondence may be addressed. E-mail: aryo@nih.go.jp or nyama@nih.go.jp.

This article contains supporting information online at www.pnas.org/cgi/content/full/0704831105/DC1.

www.pnas.org/cgi/doi/10.1073/pnas.0704831105

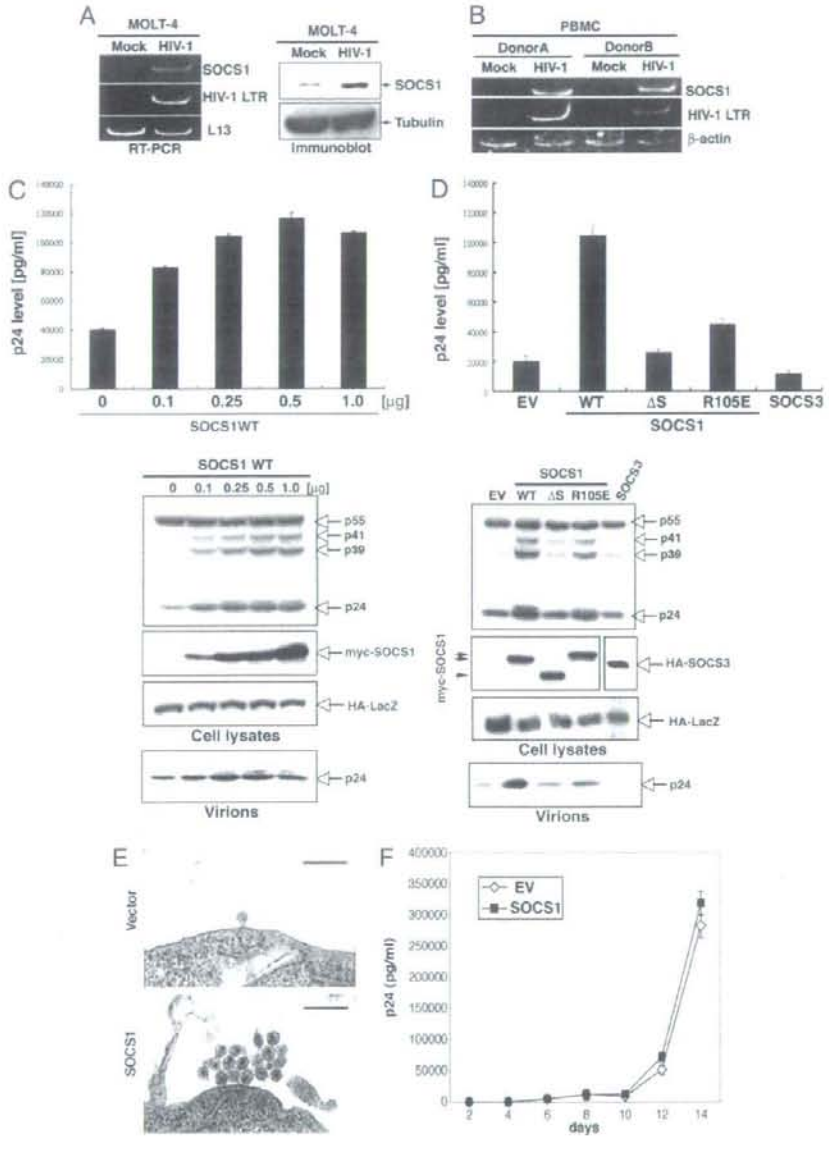

Fig. 1. SOCS1 is induced upon HIV-1 infection and enhances HIV-1 particle production. (*A*) MOLT-4 cells were mock-infected or infected with HIV-1_{NL4-3}, and then total RNA and protein extracts derived from these cells were subjected to semiquantitative RT-PCR (*Left*) and immunoblotting (*Right*), respectively. (*B*) PBMC from two healthy individuals were infected with HIV-1_{NL4-3} or were mock-infected, and SOCS1 expression was examined by semiquantitative RT-PCR. (*C*) 293T cells were transfected with pNL4-3 and cotransfected with various amounts of pcDNA-myc-SOCS1. Forty eight hours after transfection, p24 antigen release into the supernatant in each case was measured by antigen-capture ELISA (*Upper*), and the cell lysates and pelleted viruses were analyzed by immunoblotting (*Lower*). The data shown represent the mean ± SD from three independent experiments. HA-LacZ is a transfection control. (*D*) 293T cells were transfected with pNL4-3 and cotransfected with control vector, SOCS1 (WT), SOCS1ΔS (ΔSOCS box), SOCS1R105E, or SOCS3. Cell lysates and pelleted viruses were then collected after 48 h and subjected to ELISA (*Upper*) or immunoblotting (*Lower*), as described in *C*. (*E*) 293T cells cotransfected with either pNL4-3 plus control vector, or pNL4-3 plus myc-tagged SOCS1 were analyzed by TEM. Note that substantial numbers of mature virus particles can be observed in the myc-SOCS1-transfected cells. (Scale bars: 500 nm.) (*F*) Jurkat cells were infected with virions (adjusted by p24 levels) from either control vector (EV)- or SOCS1-transfected 293T cells. Supernatant p24 levels at the indicated time points were measured by ELISA.

bodies (Fig. 1*A*). In addition, *SOCS1* was found to be up-regulated also in peripheral blood mononuclear cells (PBMC) from two different individuals (following HIV infection, Fig. 1*B*).

Our initial findings that SOCS1 is induced upon HIV-1 infection prompted us to examine whether this gene product affects viral replication. We first cotransfected 293T cells with a HIV-1 infectious molecular clone, pNL4-3 (13), and also pcDNA-myc-SOCS1, and then monitored the virus production levels in the resulting supernatant. We then performed ELISA using an anti-p24 antibody and found that wild-type SOCS1 significantly increases the production of HIV-1 in the cell supernatant in a dose-dependent manner (Fig. 1*C Upper*). In contrast, neither the SH2 domain-defective mutant (R105E) nor the SOCS box deletion mutant (ΔS) of SOCS1 could promote virus production to the same levels as wild type, indicating that both domains are required for this enhancement (Fig. 1*D Upper*). Furthermore, another SOCS box protein, SOCS3, failed to augment HIV-1 replication in a parallel experiment (Fig. 1*D Upper*), indicating that the role of SOCS1 during HIV-1 replication is specific.

We next performed immunoblotting analysis using cell lysates and harvested virus particles in further parallel experiments (Fig. 1 *C* and *D Lower*). Consistent with our ELISA analysis, the expres-